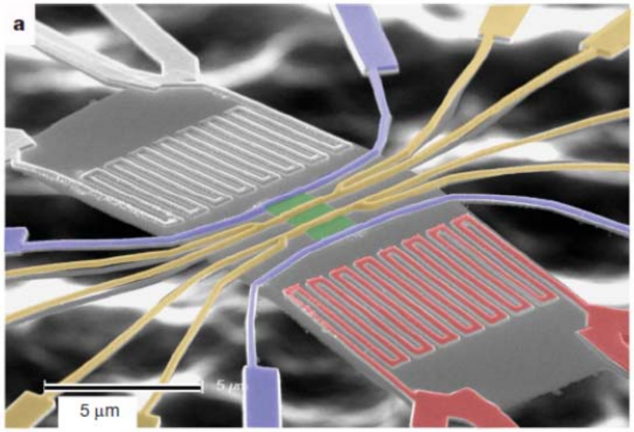

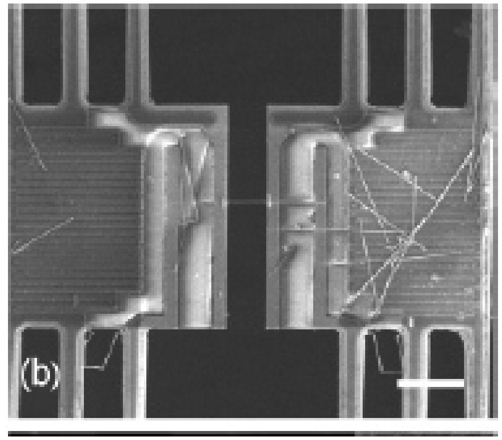

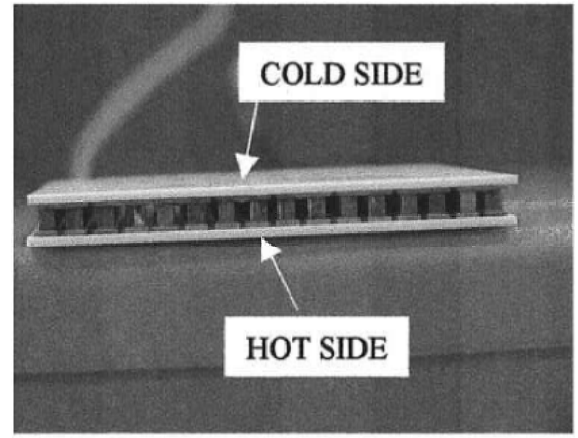

Nanomaterials for Thermoelectric Applications

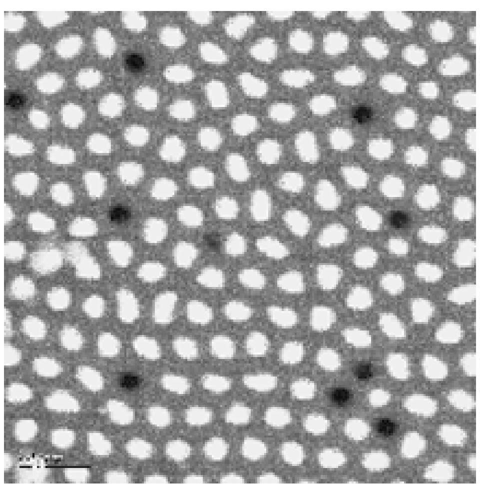
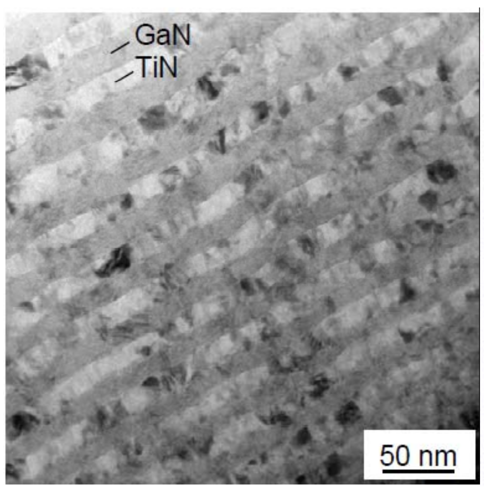

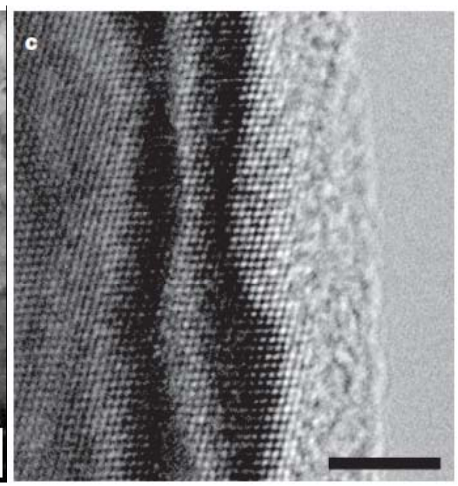

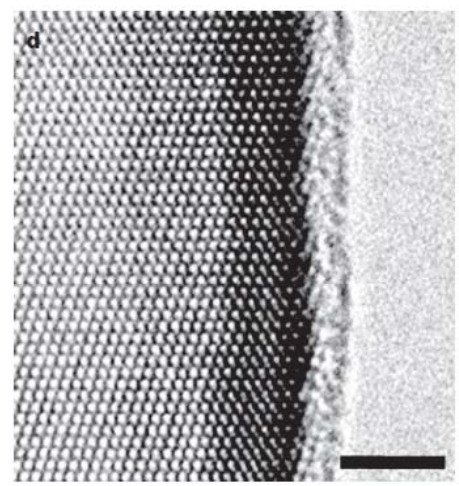

Renewable Energy

Renewable Energy Consumption by Source

US DOE - EIA Annual Energy Survey 2006

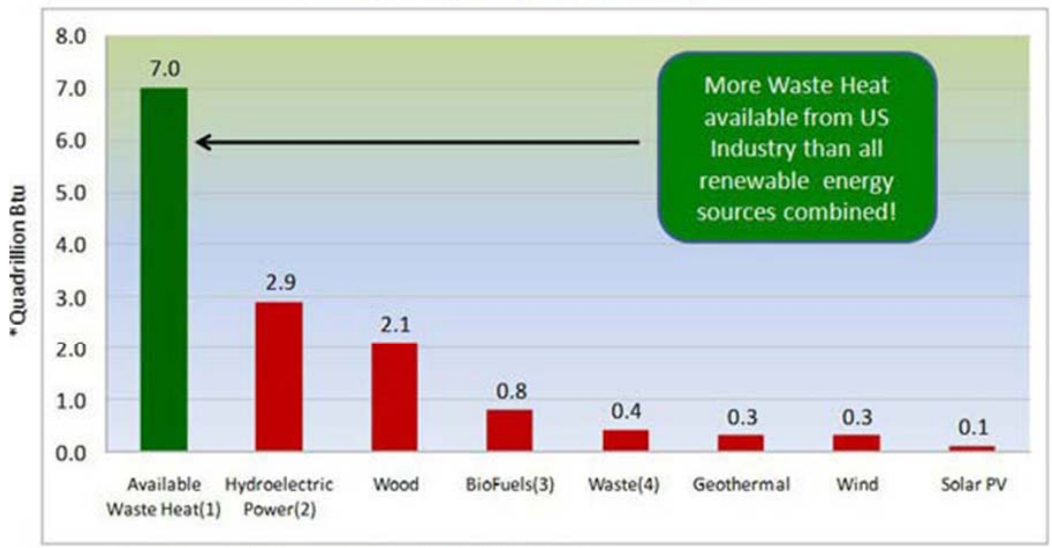

*One Quadrillion Btu is equal to one US football field 3.5 miles high of oil

1) 24.7 Quads of energy is used by industry – of this 20-50 percent is lost in the form of Waste Heat (US DOE)
2) Conventional hydroelectric power.
3) Fuel ethanol and biodiesel consumption, plus losses and co-products from the production of fuel ethanol and biodiesel.
4) Municipal solid waste from biogenic sources, landfill gas, sludge waste, agricultural byproducts, and other biomass. Through 2000, also includes non-renewable waste (municipal solid waste from non-biogenic sources, and tire-derived fuels).

- Solar
- Wind
- Water
- Biomass
- Geothermal
- Hydrogen & Fuel Cells

Exhaust Waste Heat to Electrical Power

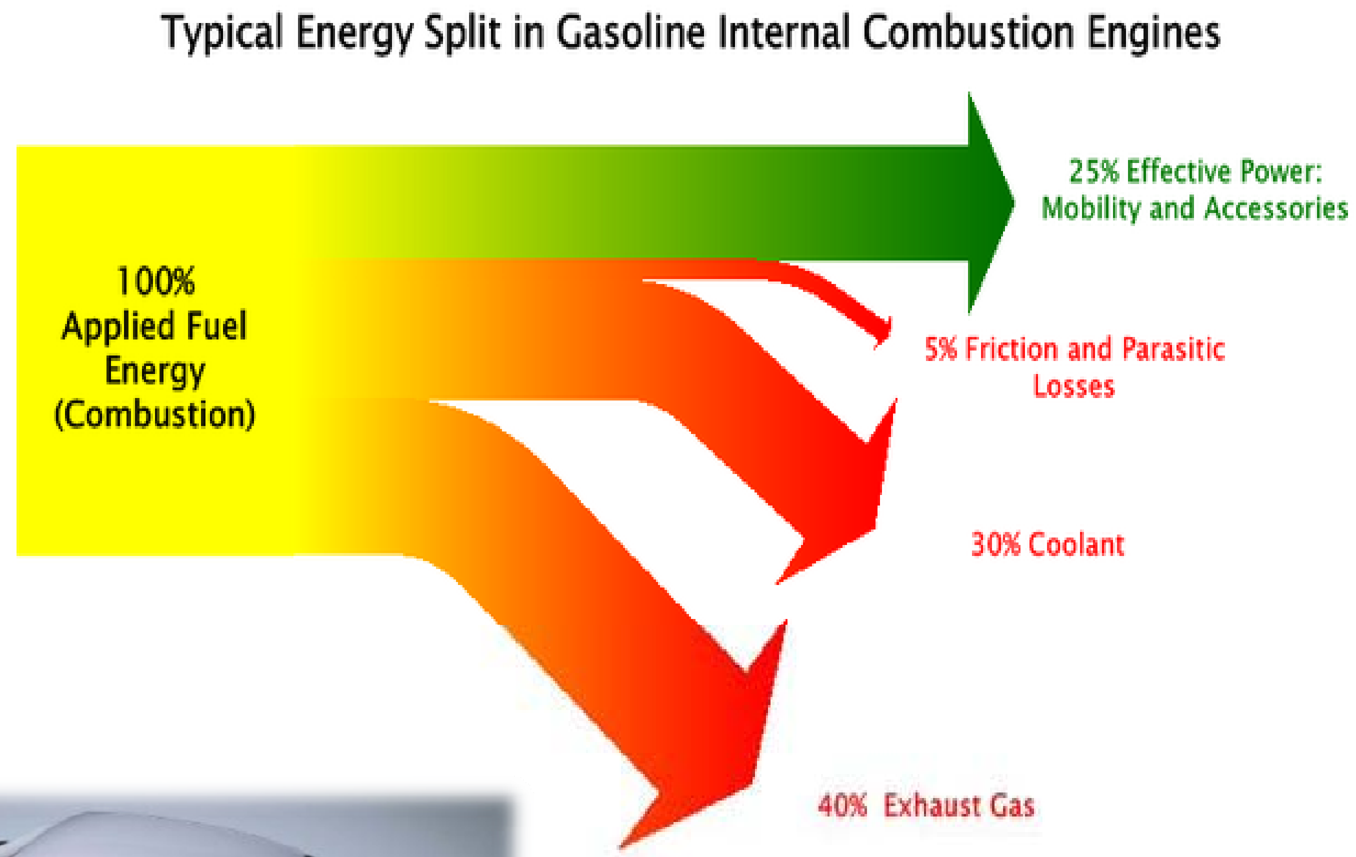

GM has 350Watt avg systems on a truck can get 3% to 4% fuel saving with better integration.

www.greencarcongress.com/thermoelectrics

The Seebeck Effect (1821)

The voltage difference, V, produced across the terminals of an open circuit made from a pair of dissimilar metals.

A. Initially, carrier (electrons or holes) move from hot to cold
B. Resulting potential difference opposes further current flow
C. The open circuit voltage is proportional to ΔT.

$$\lim_{\Delta T \to 0} \{\Delta V\} = S\Delta T$$

where *S* is the Seebeck coefficient [V/K]

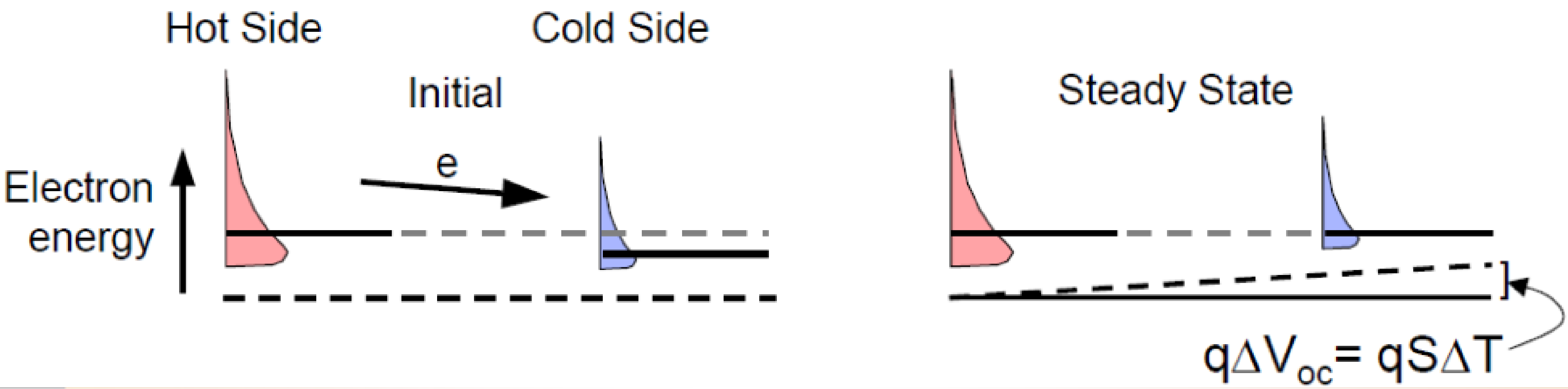

TE Generator Working Principle

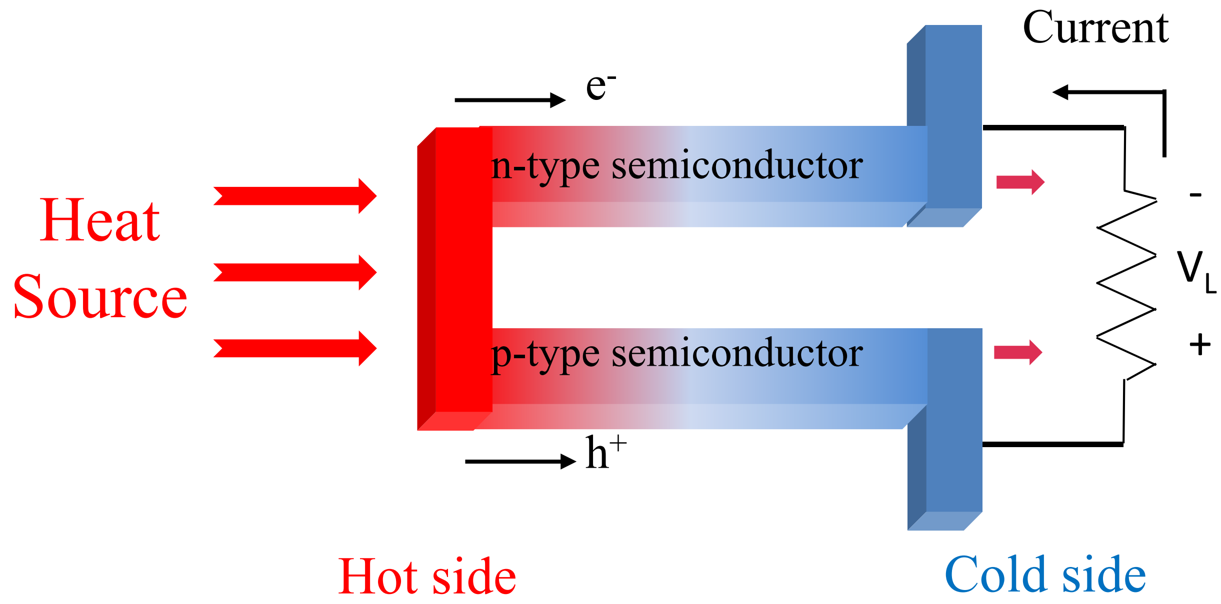

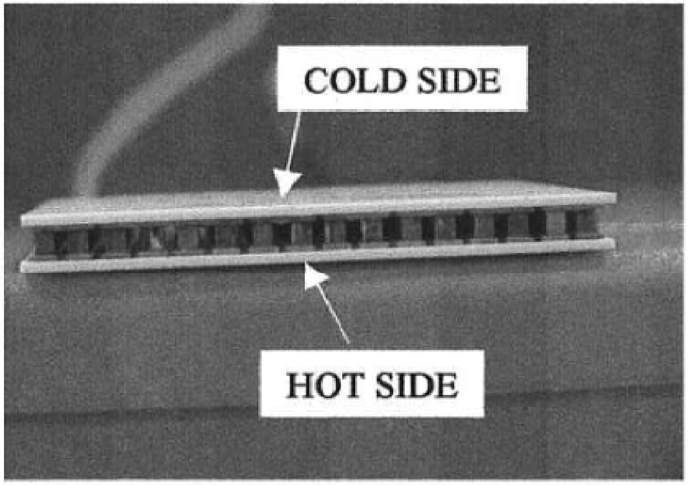

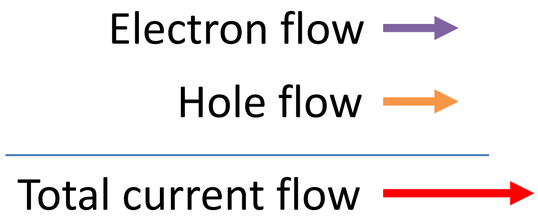

Chen et al., Intl. Mater. Rev. 48(2003)45

TE Generator Working Principle

The Seebeck and the Peltier Effect

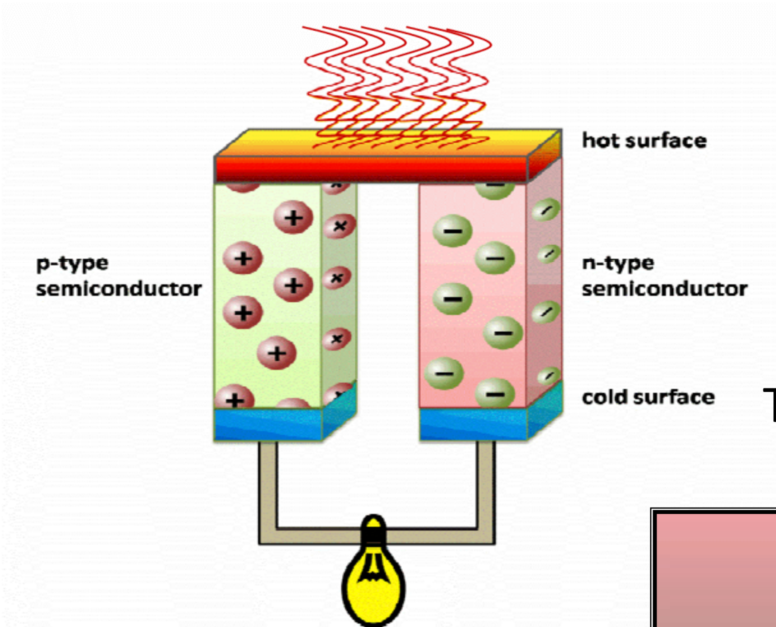

Thermoelectric
Power Generation

Thermoelectric
Device

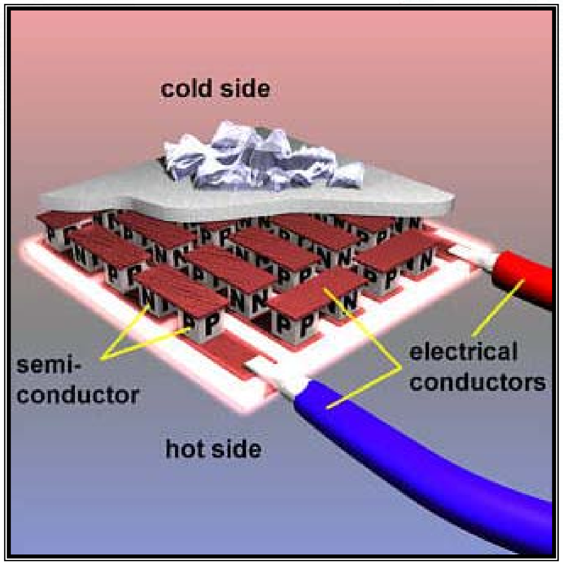

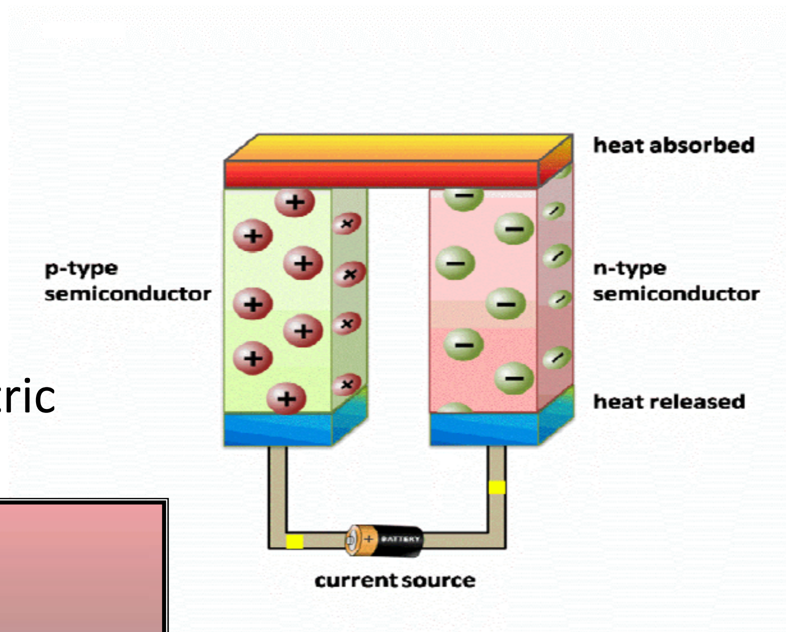

Thermoelectric
Cooling

The Peltier Effect (1834)

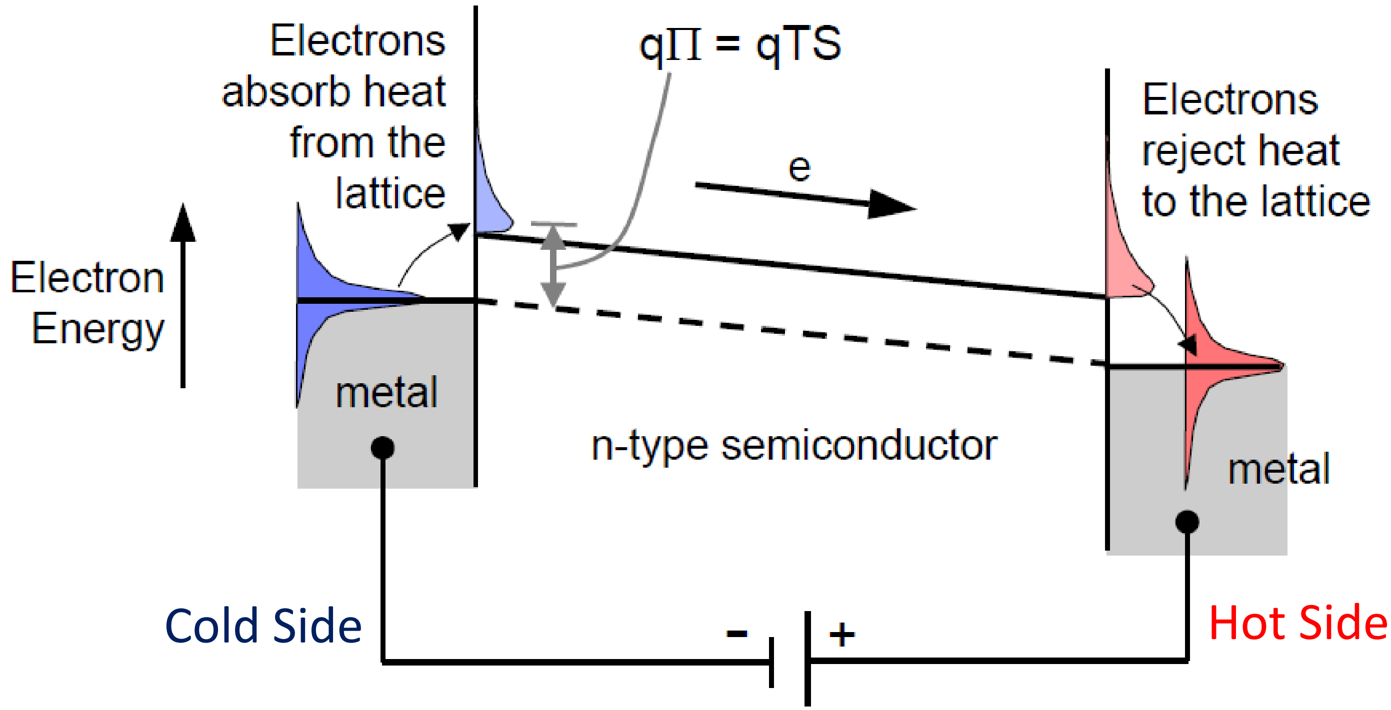

Driven by an applied potential, electrons (holes) absorb heat from the lattice at the cold side, and reject heat to the lattice at the hot side →Refrigeration.

Benefits of Thermoelectric devices

- ✓ No moving elements
- ✓ No working fluids and gases
- ✓ Low-noise operation
- ✓ Reduced size and weight
- ✓ High reliability — KRYOTHERM guarantees lifetimes of more than 200,000 hours for our TEDs
- ✓ Easy switching from cooling to heating mode

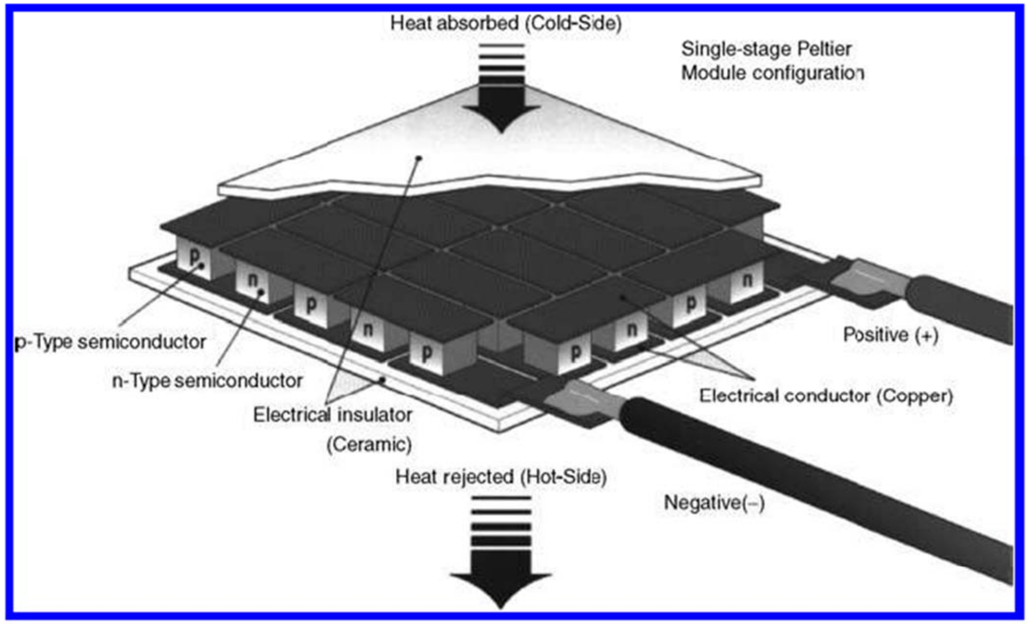

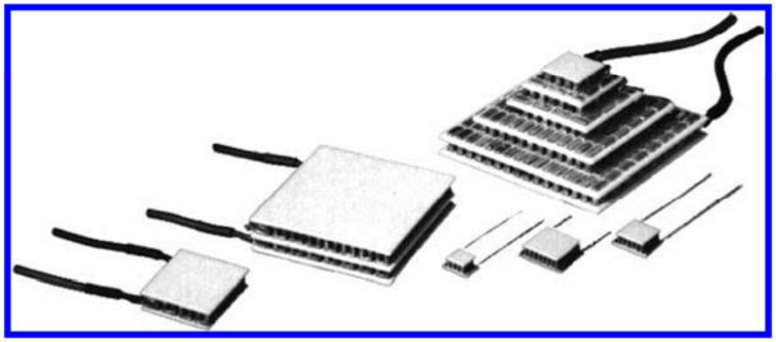

Example of TE Devices: Voyagers

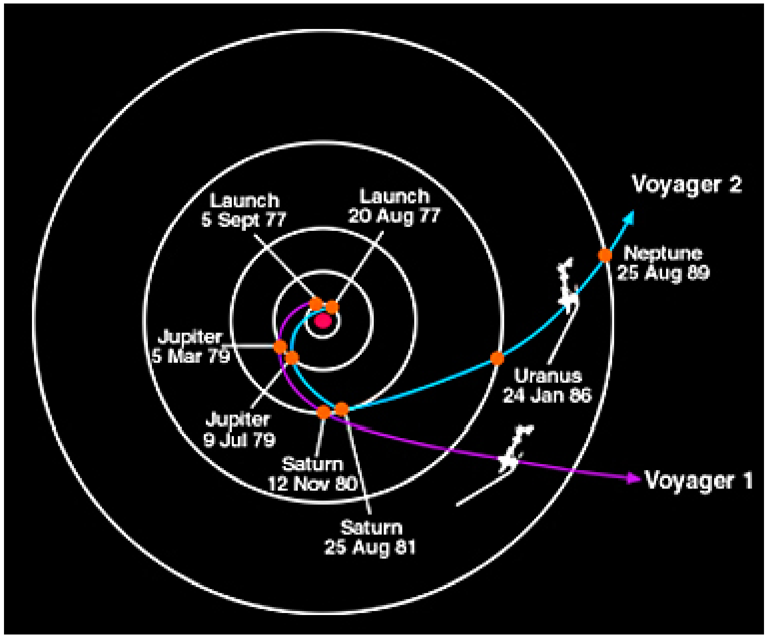

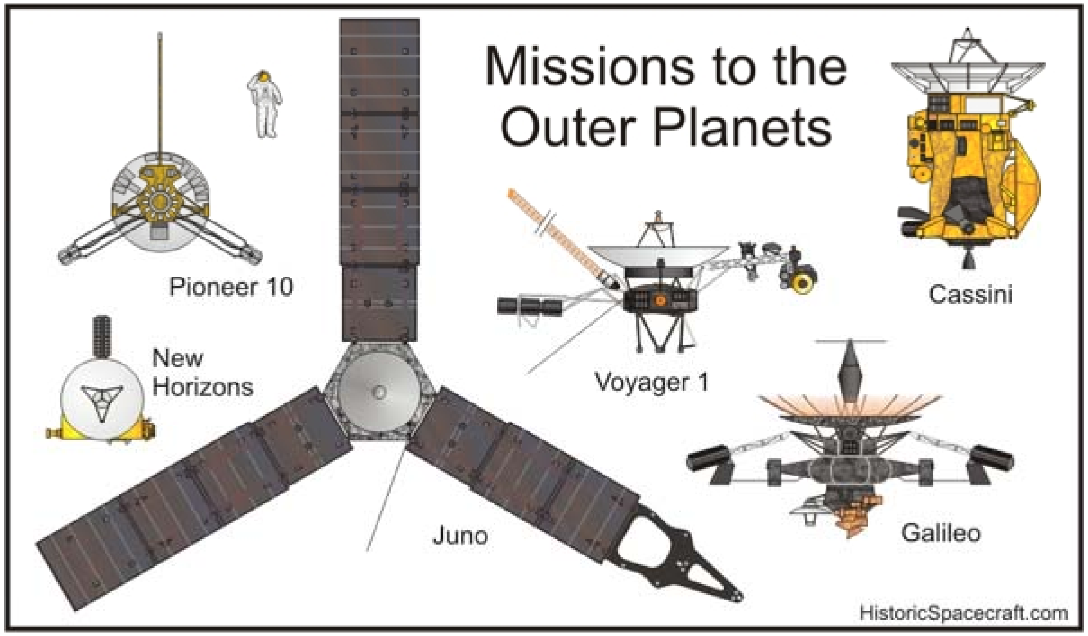

Example of TE Devices: RTG

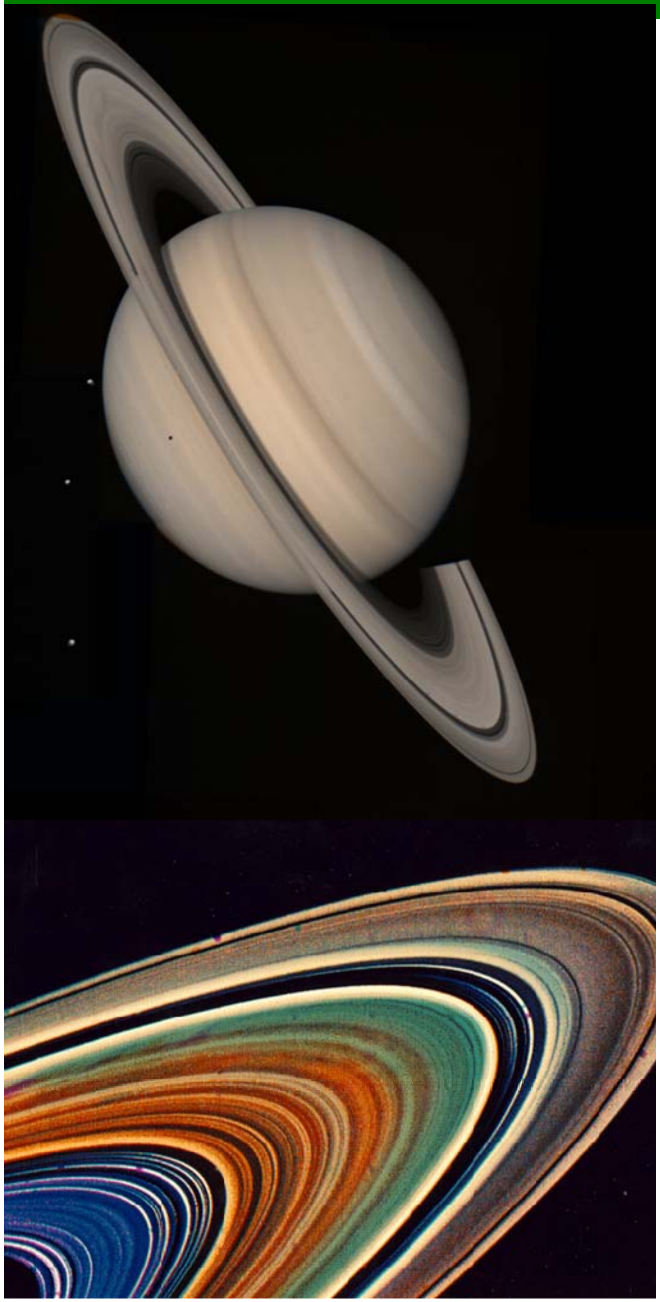

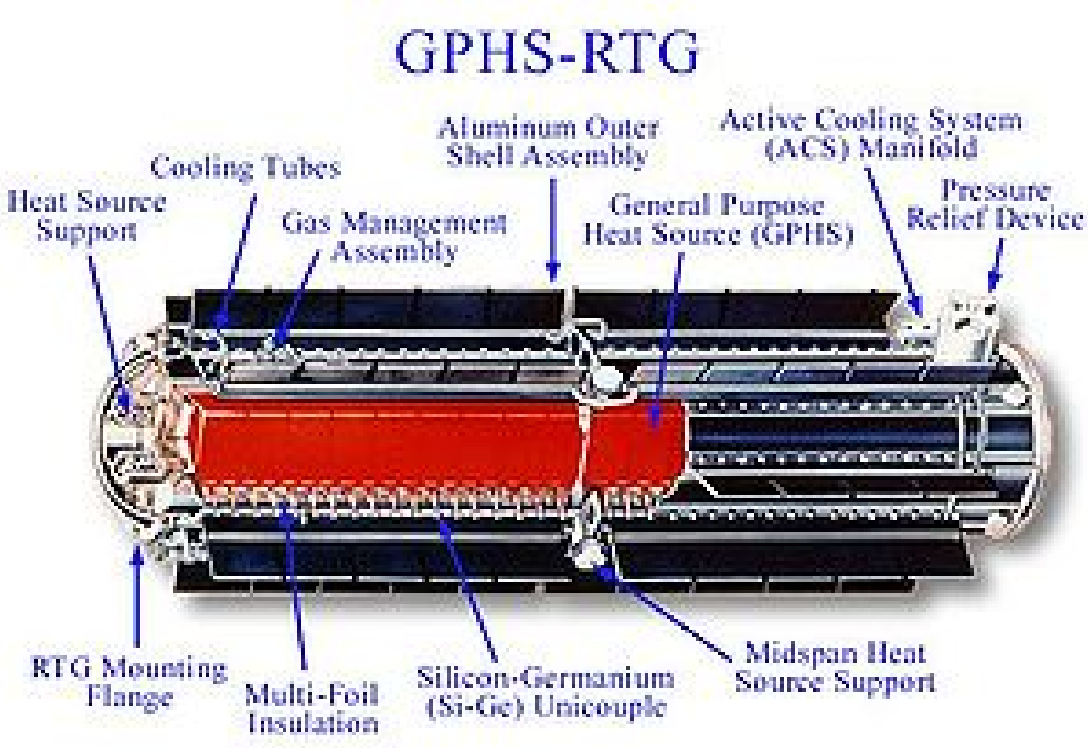

Radioisotope thermoelectric generator (**RTG**, **RITEG**)

Example of TE Devices: CCD Cooling

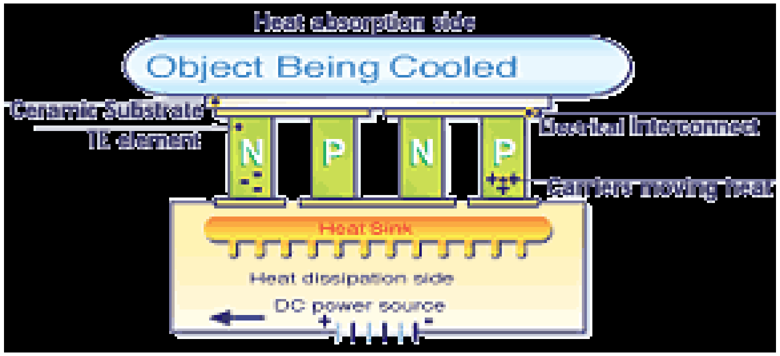

Koolatron P-27 Voyager - A Thermoelectric Cooler - 12 Volt Cooler ($139.95)

Thermoelectric Efficiency and the Figure-of-Merit

The efficiency of the generator is given by

$$\phi = \frac{\textit{energy supplied to the load}}{\textit{heat energy absorbed at hot junction}}$$

q is the heat input required at the hot junction. Consider three effects:

1. Peltier heat $q_1 = -\pi I$

2. A portion of the Joule heat (It is assumed that both elements are of equal length and that element b has unit cross-sectional area.)

$$q_2 = -(\frac{I^2}{2})[\rho_b + (\rho_a/A)]L$$

3.Heat conducted away from the hot junction by thermal conduction

$$q_3 = (\kappa_b + A\kappa_a)\Delta T/L$$

$$(q_H = -\kappa \nabla T)$$

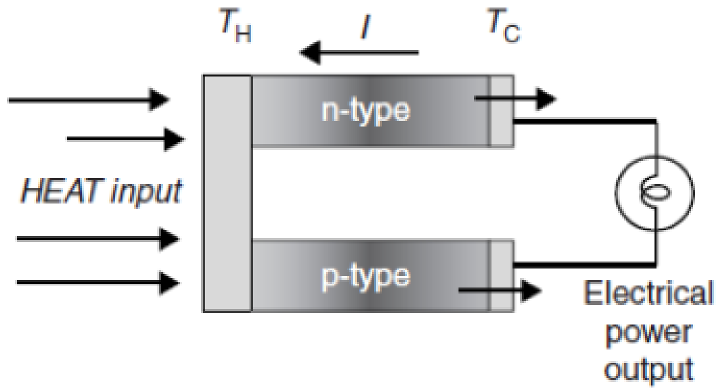

The Seebeck effect (Thermoelectric generation)

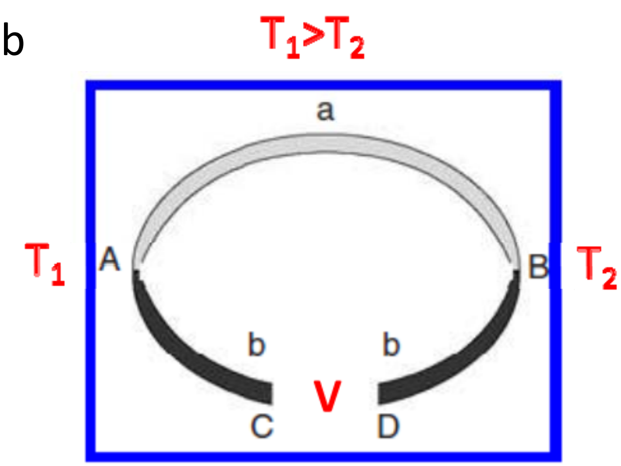

Schematic basic thermocouple.

$$\eta = \frac{I^2 R_L}{\left\{(\kappa_b + \kappa_a A)\left(\frac{\Delta T}{L}\right) - \left(\frac{I^2}{2}\right)\left[\rho_b + \left(\frac{\rho_a}{A}\right)\right] L - \pi I\right\}}$$

Where $I = \frac{V_L}{R} - \frac{S_{ab}\Delta T}{\left\{R_L + \left[\rho_b + \frac{\rho_a}{L}\right] L\right\}}$

$$\eta = \left(\frac{\Delta T}{T_H}\right)\left[\frac{\sqrt{1 + Z\bar{T}} - 1}{\sqrt{1 + Z\bar{T}} + \frac{T_c}{T_h}}\right]$$

The efficiency of the device is limited by the Carnot efficiency ($\Delta T/T_H$)

and $\bar{T} = \frac{T_H + T_L}{2}$

and $Z = \frac{S^2}{\left[\sqrt{\frac{\kappa_b}{\rho_b}} + \sqrt{\frac{\kappa_b}{\rho_b}}\right]^2}$ is called the Figure of merit.

In practice, the two arms of the junction have similar material constants, in which case the concept of a figure-of-merit for a material is employed and given by

$$Z = \frac{S^2 \sigma}{\kappa}$$

S : Seebeck coefficient
T : absolute temperature
σ: electrical conductivity
κ : thermal conductivity

Differential Electron Conductivity

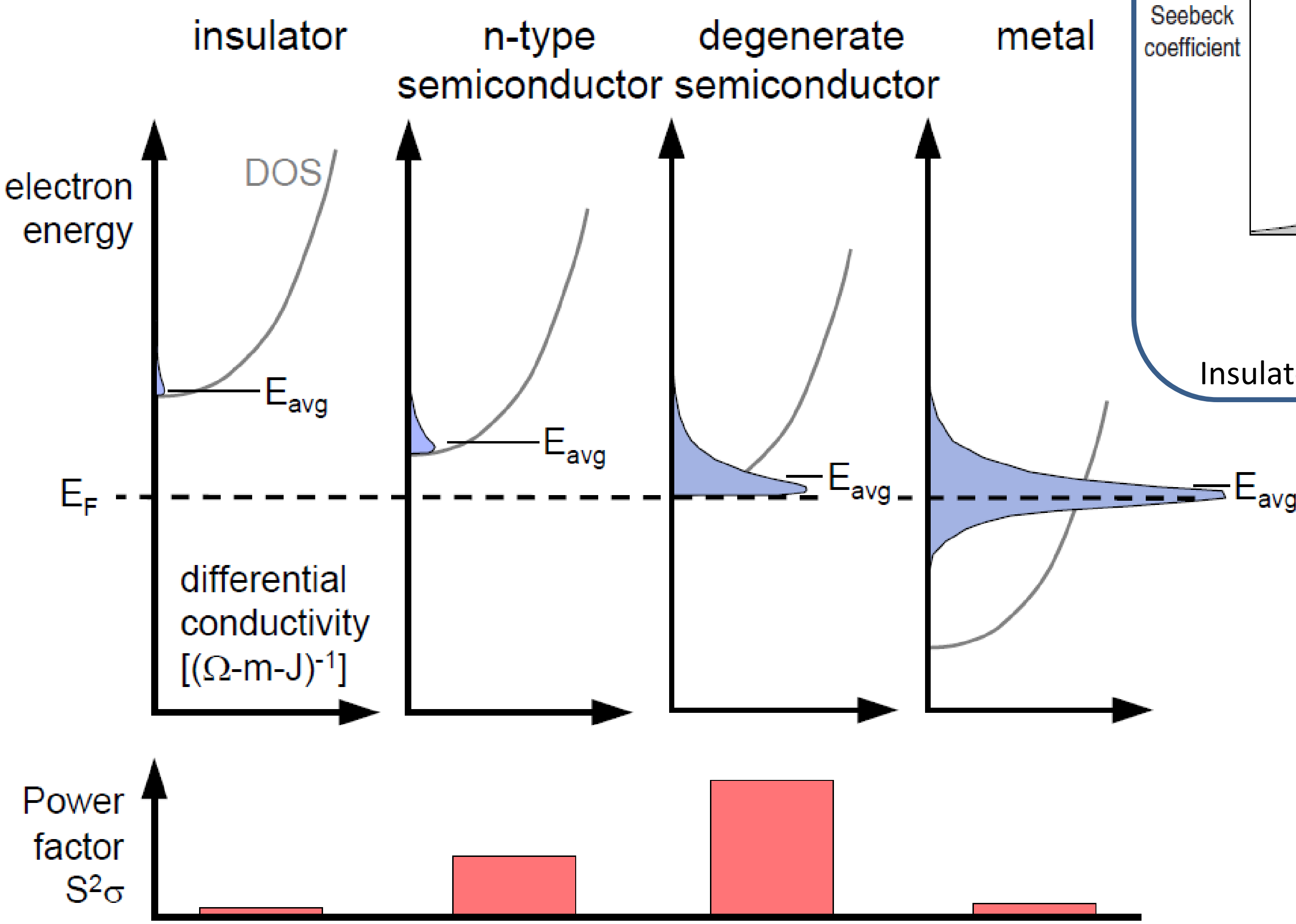

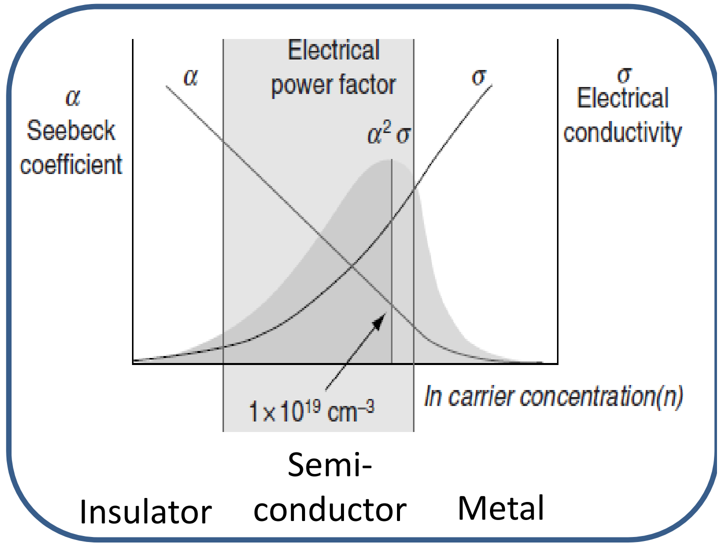

"Power factor"

$$ZT = \frac{S^2\sigma}{k}T$$

Selection of Thermoelectric Materials

$$Z = \frac{S^2\sigma}{\kappa}$$

Electrical conductivity σ
Thermal conductivity κ
Seebeck coefficient S

Free carrier density n

The thermal conductivity

$$\kappa = \kappa_{Lattice} + \kappa_{Electron}$$

Lattice part is roughly independent of n while the electronic part is directly related to the electrical conductivity

High power factor, Low thermal conductivity

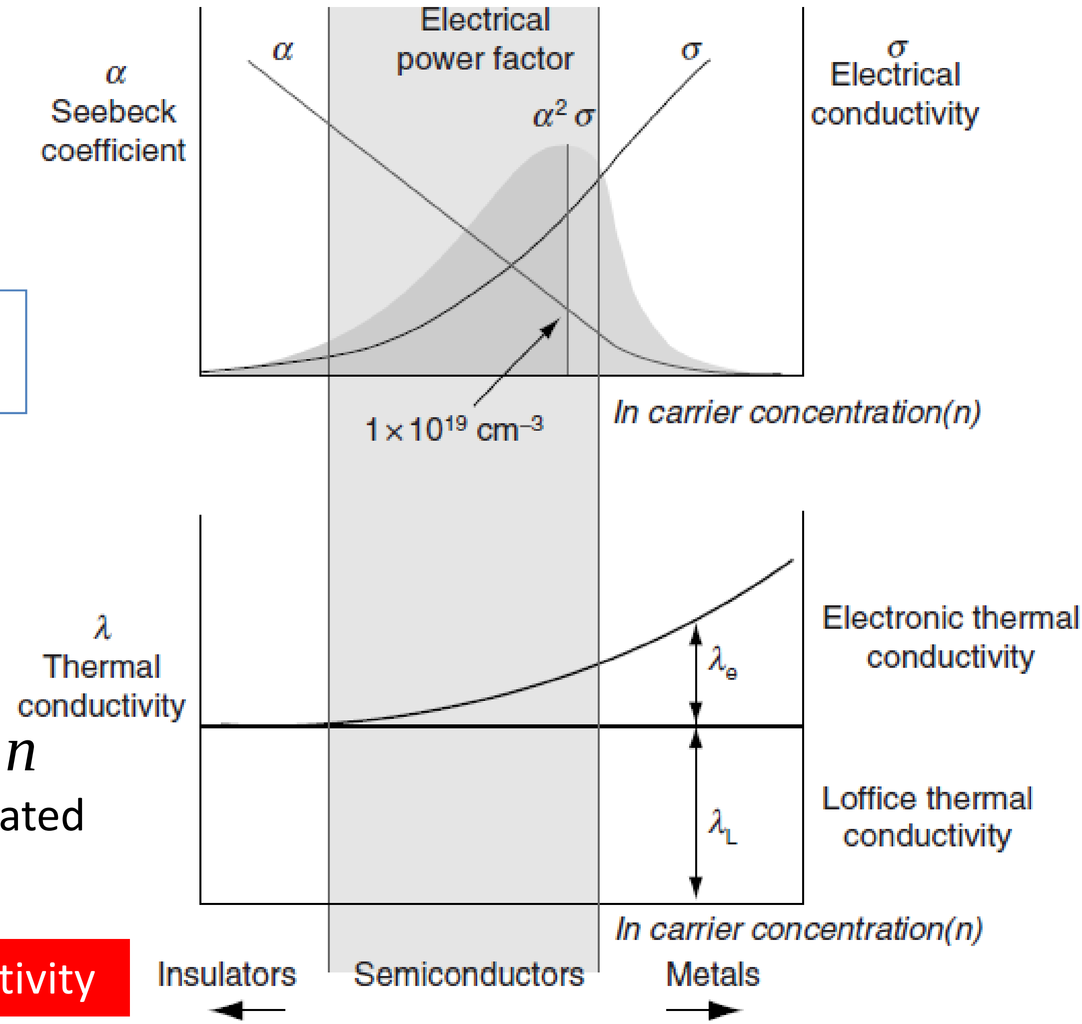

Schematic dependence of electrical conductivity, Seebeck coefficient, power factor, and thermal conductivity on concentration of free carriers.

ZT in This Decade

Year	Journal	Materials	ZT	T(K)	Institute
2011	Nature	$PbTe_{1-x}Se_x$ (Buck)	1.8	850K	MS, California Institute of Technology
2009	Nature	In_4Se_{3-d} (Buck)	1.5	700K	Samsung
2008	Nature	Si (52nm rough NWs)	0.6	300K	Berkeley
2008	Nature	Si (20nm NWs)	1.0	200K	CE, California Institute of Technology
2008	Science	BiSeTe (buck)	1.5	400K	Physics, Boston College
2004	Science	$AgPb_mSbTe_{2+m}$ (buck)	2.1	800K	Michigan State University
2003	Nature	Bi_2Te_3/Pb_2Te_3 SL	2.6	300K	Research Triangle Institute
2002	Science	PbSeTe/PbTe SL	1.6	300K	Massachusetts Institute of Technology
Before			~1		

Y. Z Pei et al, Nature 473, 66 (2011)
J. S. Rhyee et al, Nature 459, 965 (2009)
A. I. Hochbaum et al, Nature 451, 163 (2008)
A. I. Boukai et al, Nature 451, 168 (2008)
B. Poudel et al,Science 320, 634 (2008)
K. F. Hsu et al, Science 303, 818 (2004)
R. Venkatasubramanian et al, Nature 413 597 (2003)
T. C. Harman et al, Science 297, 2229 (2002)

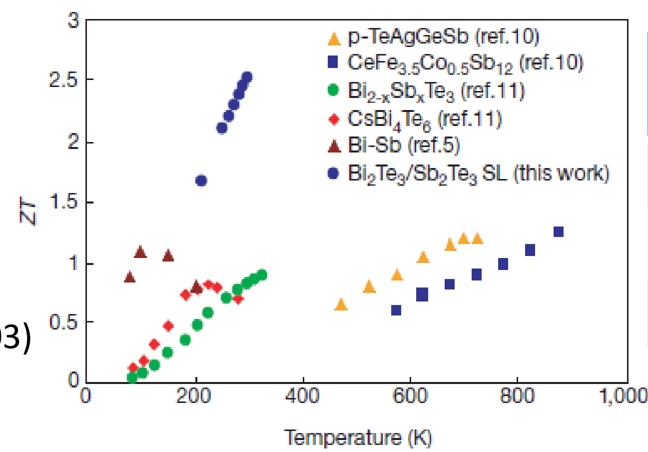

Nature Materials	Publication
2011	4
2010	4
2003-2009	13

ZT & Efficiency

Efficiency η

$$\eta = \frac{T_H - T_C}{T_H} \frac{\sqrt{1+ZT} - 1}{\sqrt{1+ZT} + T_C/T_H}$$

Figure-of-merit *ZT*

$$ZT = T\frac{S^2\sigma}{\kappa}$$

Thermal conductivity k

$$\kappa = \kappa_L + \kappa_{el}$$

Efficiency examples

ZT	T_H/K	T_C/K	η
0.5	673	373	5.6%
1	673	373	9.4%
2	673	373	14.3%
3	673	373	17.4%
3	773	373	20.8%
3	873	373	23.6%

Thermal conductivity k

$$\kappa_{el} = L_0 \sigma T$$

- To match a refrigerator, an effective ZT= 4 is needed
- To efficiently recover waste heat from car, ZT = 2 is needed

ZT & Efficiency

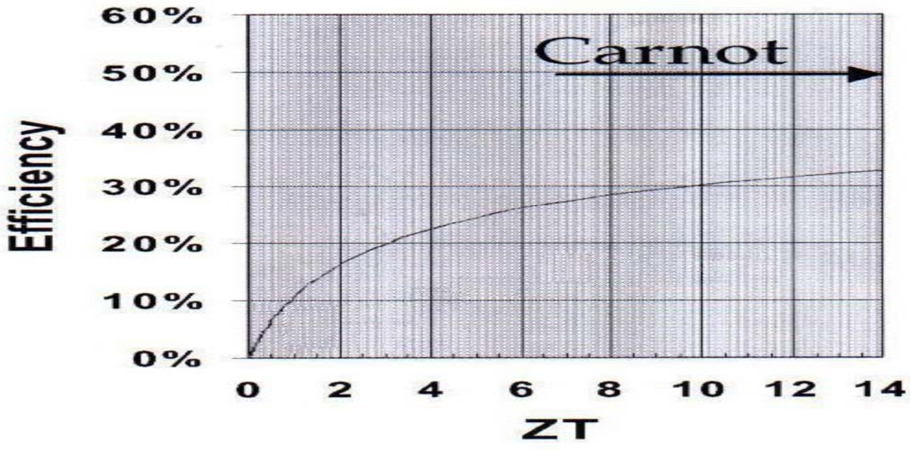

Efficiency for $T_c / T_h = 0.5$

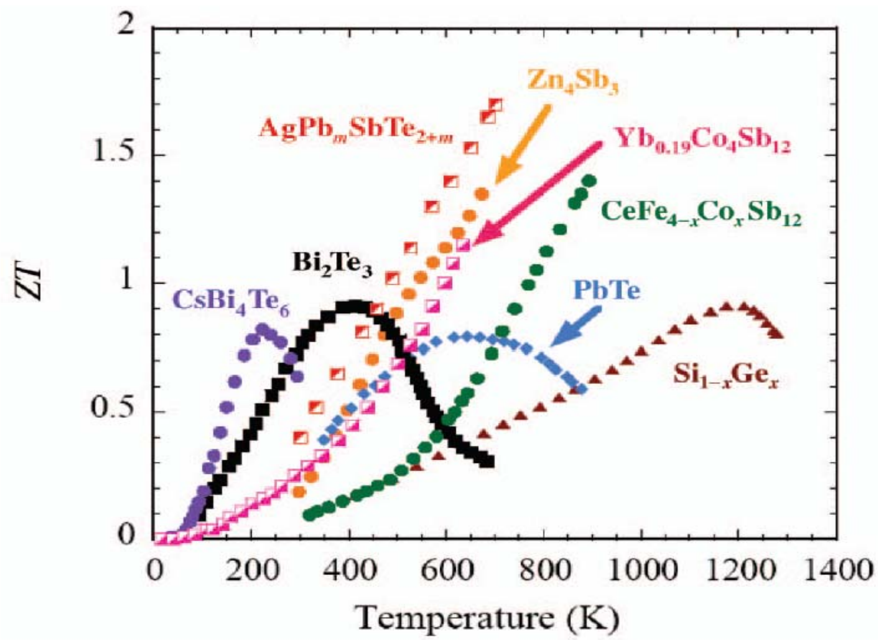

ZT > 2.4 @ 300K

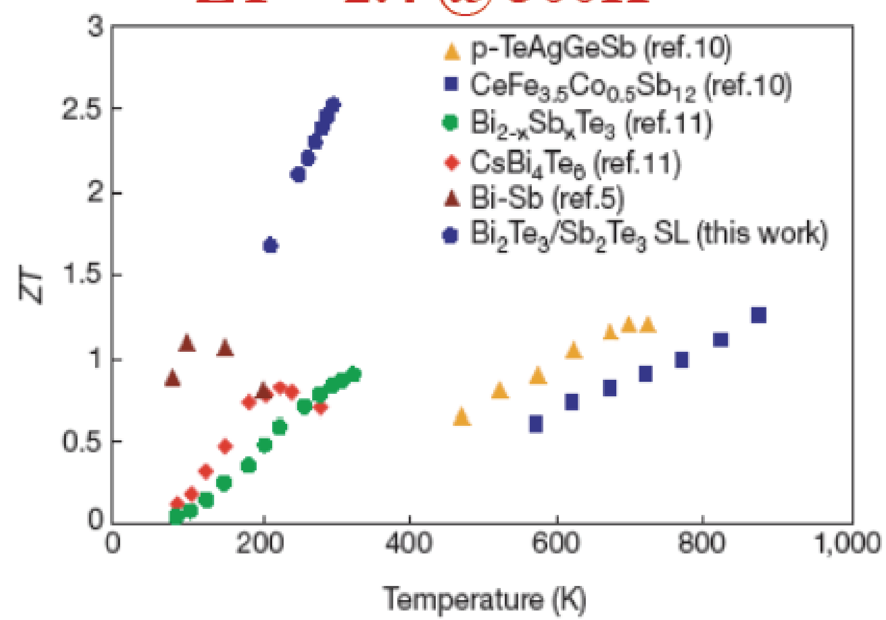

TE Device with Superlattice Structure

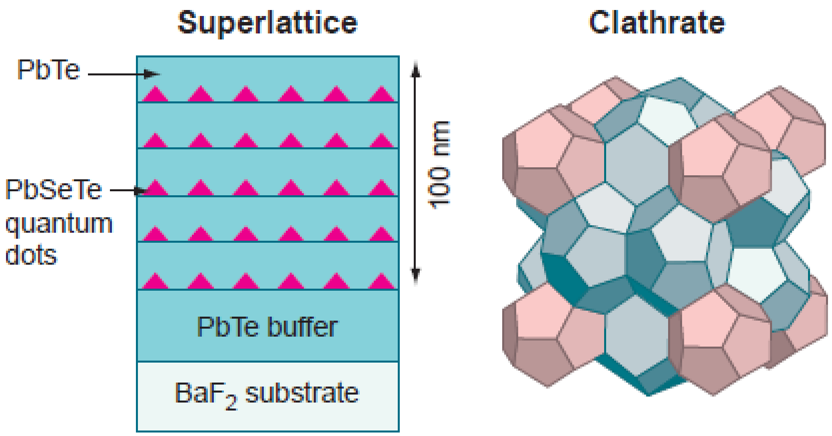

Promising new materials. (Left) Nanoengineered thermoelectric materials of this kind are prepared with molecular beam epitaxy. **(Right)** In this model clathrate crystal structure, the cubic crystal structure is composed of two types of polyhedra that consist of clusters of 20 or 24 atoms. In self-assembled structures of this type, nature does the nanoengineering.

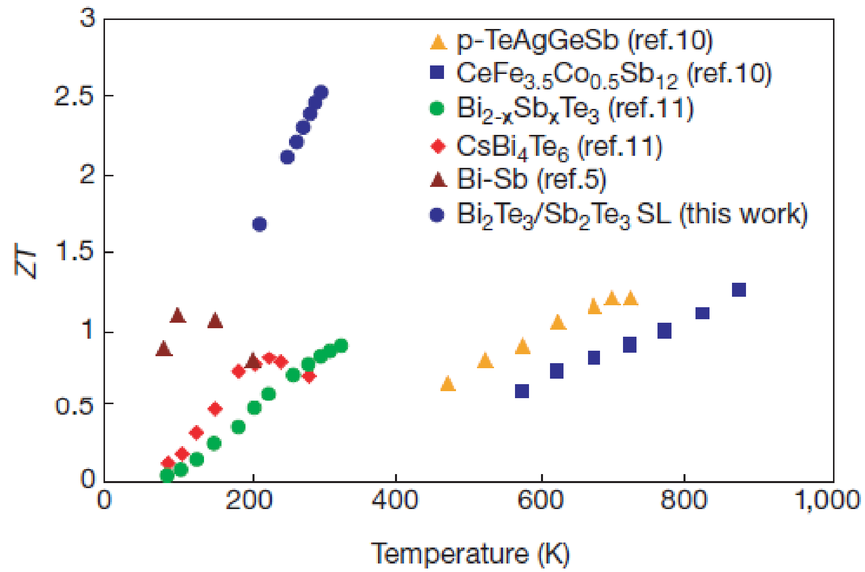

Table 1 Theoretical and experimental lattice thermal conductivities

Material	Thermal conductivity ($W\,m^{-1}\,K^{-1}$)
K_{min} of Bi_2Te_3 (*a-b* axis), Slack model[34]	0.55
K_{min} of Bi_2Te_3 (*c* axis), Slack model[34]	0.28
K_{min} of Bi_2Te_3 (*a-b* axis), Cahill model[35]	0.28
K_{min} of Bi_2Te_3 (*c* axis), Cahill model[35]	0.14
K_L of $Bi_{2-x}Sb_xTe_3$ alloy (*a-b* axis)	0.97
K_L of $Bi_{2-x}Sb_xTe_3$ alloy (*c* axis)	0.49
K_L of Bi_2Te_3/Sb_2Te_3 superlattice (*c* axis)	0.22

Lattice thermal conductivity (K_L) of the Bi_2Te_3/Sb_2Te_3 superlattice (period ~50 Å) compared with K_L observed in the respective alloys and the theoretical minimum lattice thermal conductivity (K_{min}) from various models.

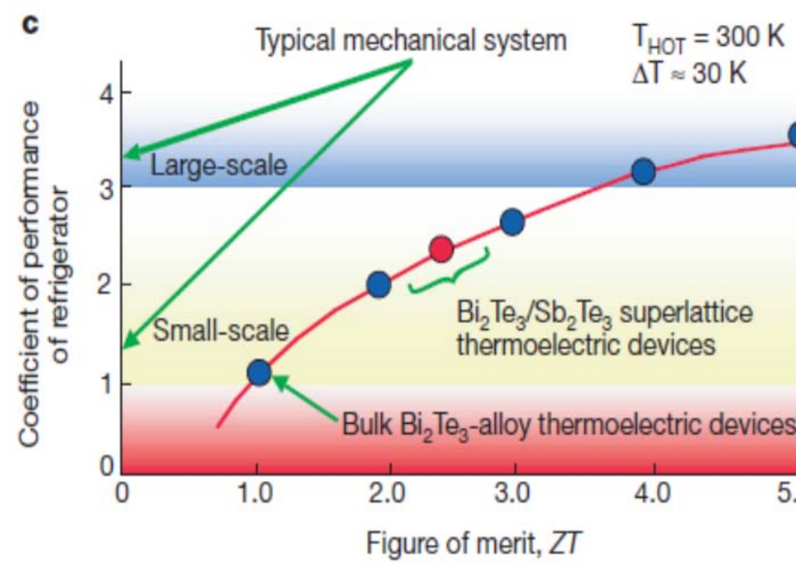

Efficiency and *ZT*

$$\eta_{TE} = \eta_C \left(\frac{\sqrt{1+ZT} - 1}{\sqrt{1+ZT} + \frac{T_C}{T_H}} \right)$$

Carnot efficiency, $\eta_C = (T_H - T_C)/T_H$

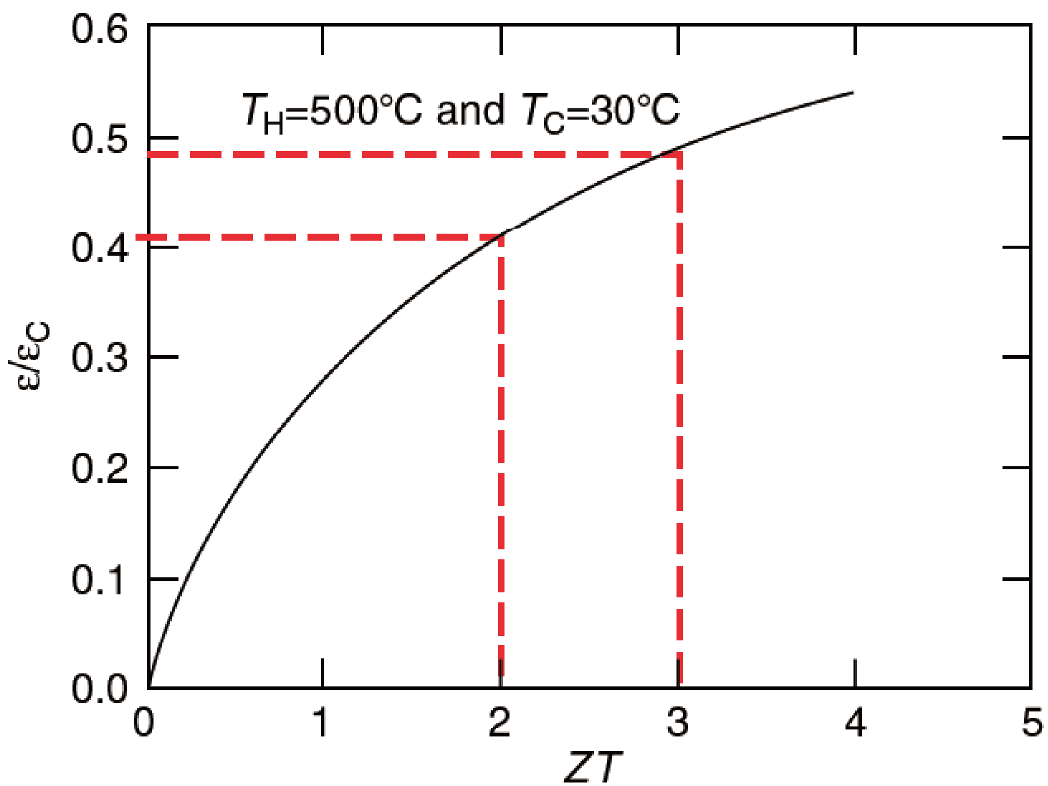

Searching for New Thermoelectric Materials

- Figure of Merit = ZT = $(\alpha^2\sigma/k)T$
  - T = Absolute Temperature
  - α^2 = (Seebeck coefficient)^2
    - Tells how much average thermal energy is transported by each carrier
  - σ = electrical conductivity
    - Tells how much the carriers can transport energy without Joule loss
  - k = thermal conductivity
    - Tells how small is the reverse flow of heat from the cold-side to the hot-side, opposing the electron-transport of heat
- <u>Minimize</u> thermal conductivity and <u>maximize</u> electrical conductivity

Can nanotechnology be adopted to minimize thermal conductivity and maximize electrical conductivity?

Searching for New Thermoelectric Materials

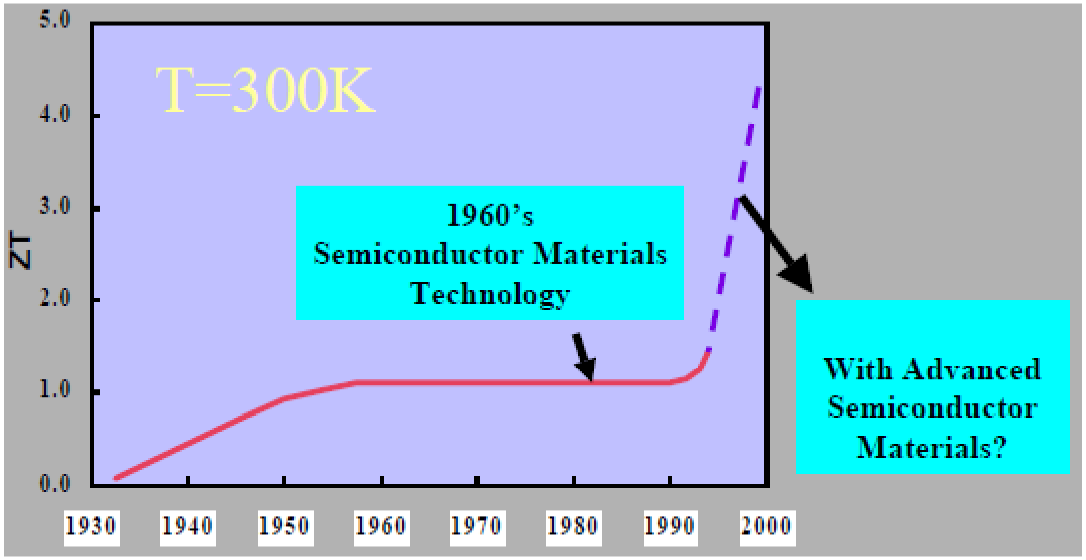

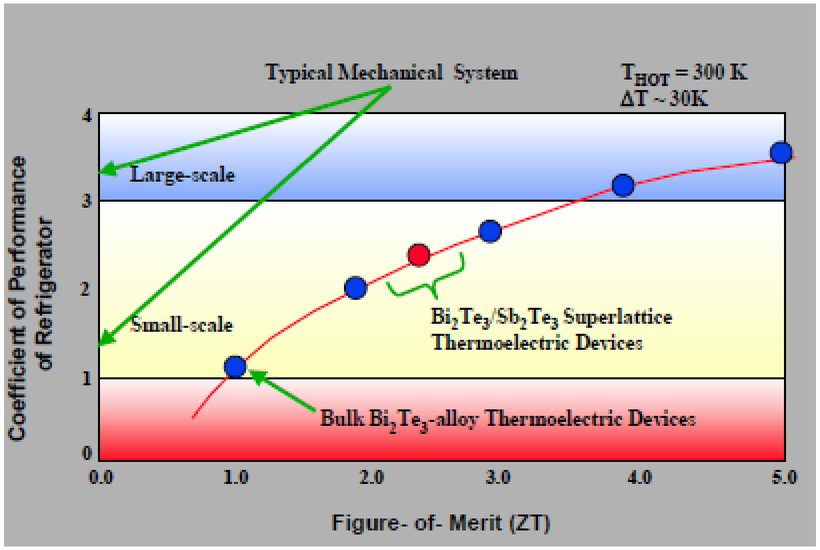

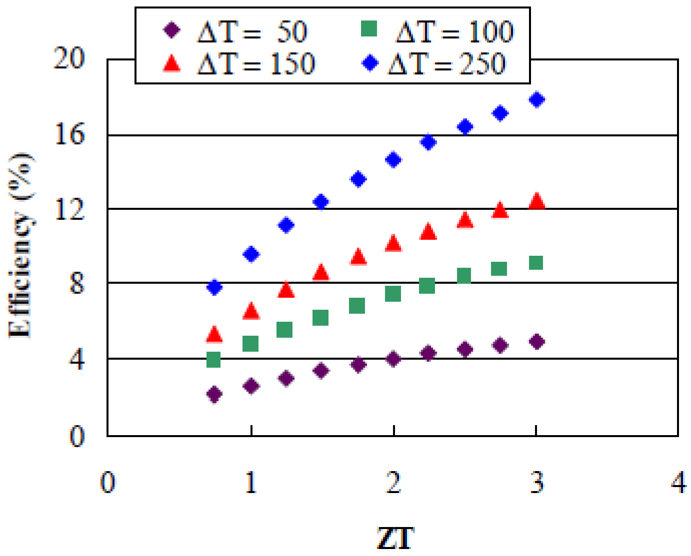

- ZT need to improve over 1.3 at 300K for a major impact in electronics cooling and around 2.5 for a revolutionary impact in air-conditioning, and power from waste-heat

New Approaches

- New Bulk Materials
  - Skutterudites (Rensselaer, Oak Ridge, JPL, 1992)
    - Cage-structures with rattling atoms to scatter phonons
  - Novel Chalcogenides and Clathrates (Michigan State and Arizona, 1994)
    - Complex Variations of Bi_2Te_3 to reduce phonon mean-free paths
- Nano-scale Materials
  - Low-Dimensional Structures (MIT, MIT Lincoln Labs, 1992)
    - Quantum-confinement to Enhance Density of states which increase Seebeck coefficient
  - Nano-scale Superlattices (RTI, 1992)
    - **Phonon-blocking** from acoustic mismatch between superlattice components but **electron-transmitting** due to negligible electron-energy offsets
  - Heterostructure Thermionics (UCSB, Oak Ridge, 1996)
    - Thermionic-like effects using energy barriers that can be controlled in hetero-structures

New Progresses

- Cs Bi_4Te_6 (Michigan State University)
  - Bulk Materials with a ZT~ 0.8 at 225K but less than 0.8 at 300K (*Science* **287**, 1024-1027, 2000)
- Filled Skuterrudites (JPL)
  - Bulk materials with a ZT ~1.35 at 900K (Proc. Of 15th International Conf. On Thermoelectrics, 1996)
- PbTe/PbTeSe Quantum-dots (Harman, MIT Lincoln Labs.)
  - ZT~ 1.6 at 300K based on cooling data (*Science* 297, Sep. 2002)
- Bi_2Te_3/Sb_2Te_3 Superlattices (RTI)
  - ZT~2.4 at 300K in devices with all properties measured at the same place, same time, with current flowing and verified by two independent techniques (*Nature*, 597-602, Oct. 2001)

Nanostructured Superlattice

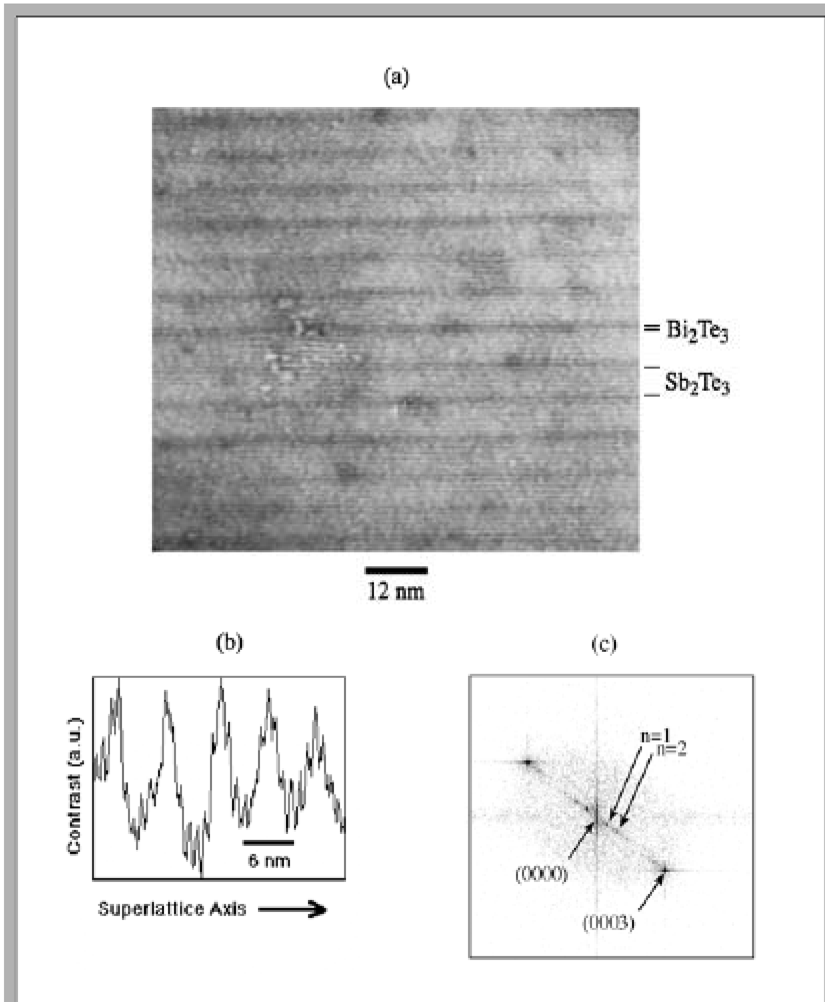

Applied Physics Letters, 75, 1104 (1999)

- 10Å/50Å Bi_2Te_3/Sb_2Te_3 Structure
- Optimized for disrupting heat transport while enhancing electron transport perpendicular to the superlattice interfaces

Lattice turning for TE

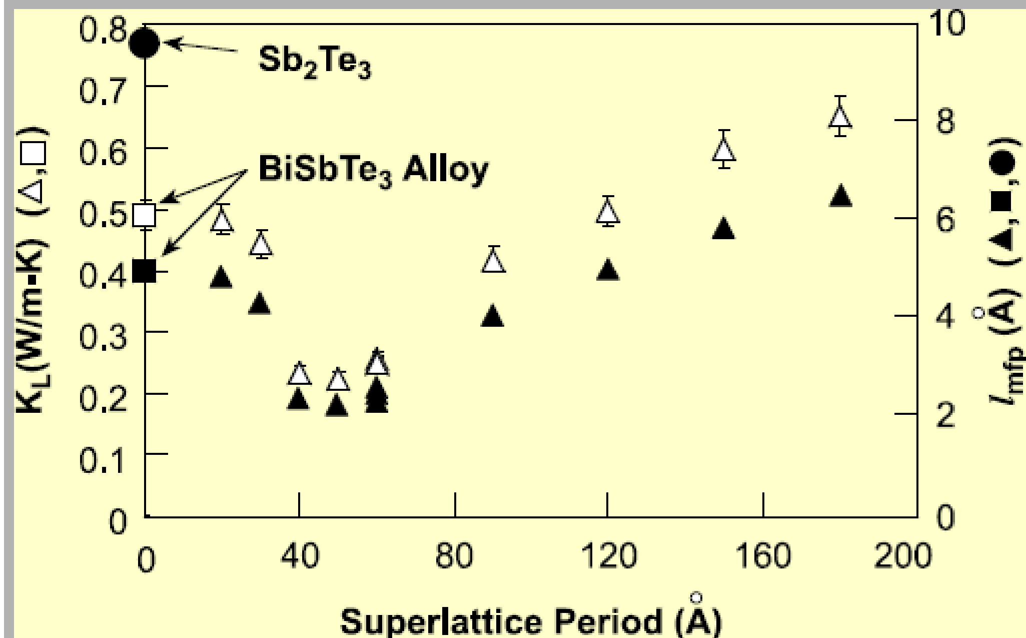

Physical Review B, 61, 3091 (2000)

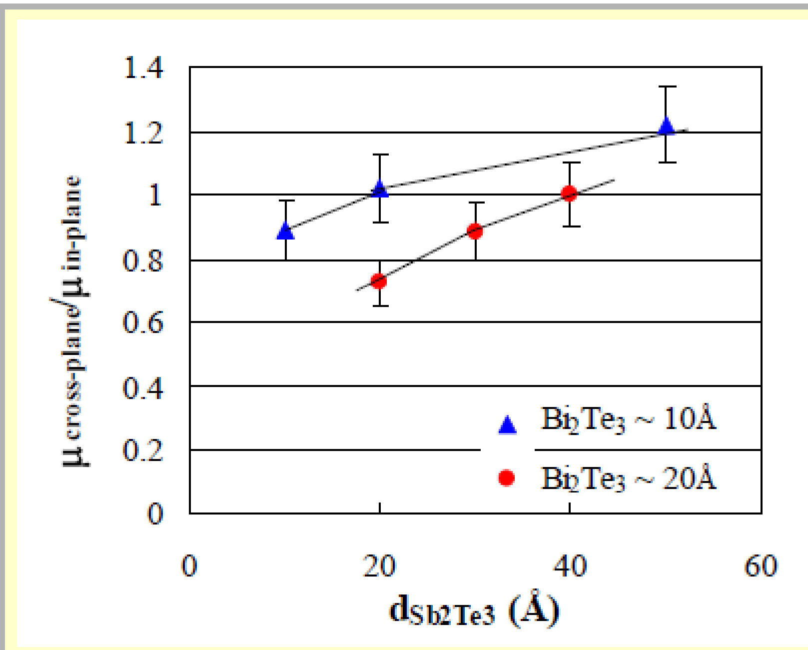

Nature, 413, 597-602 (2001)

New Ideas: Metal-Organic-Metal

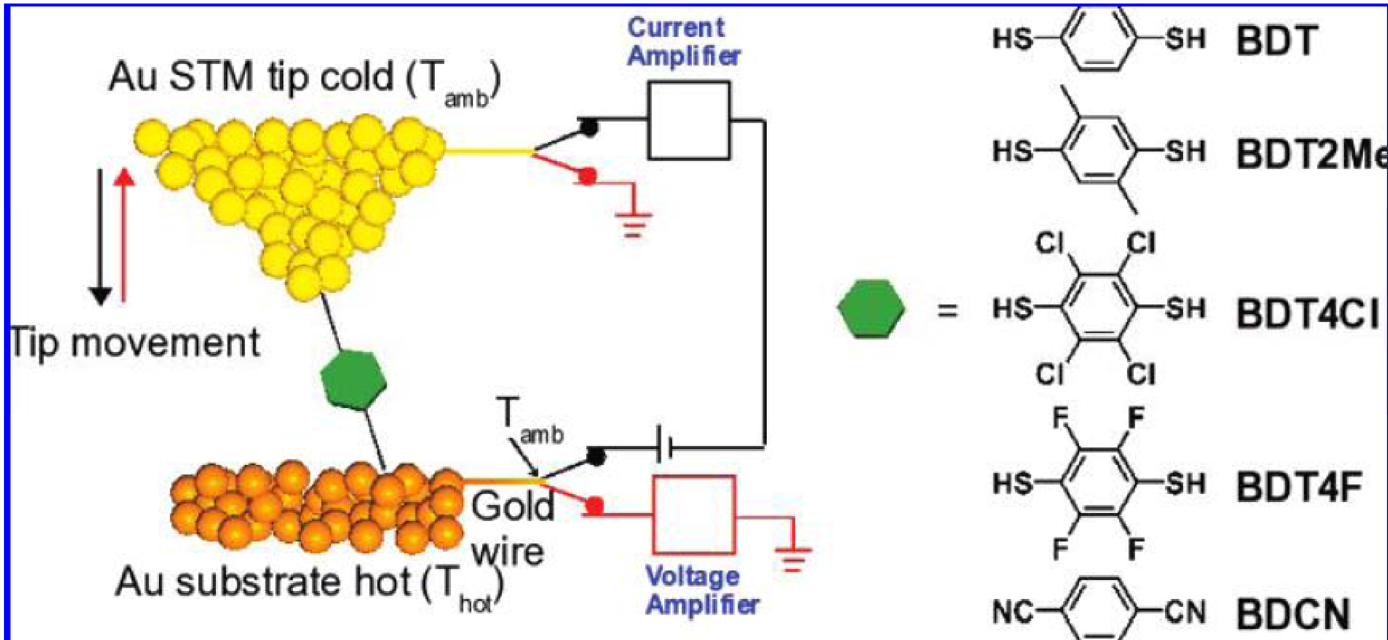

NANO LETTERS

2008
Vol. 8, No. 2
715−719

Rachel A. Segalman

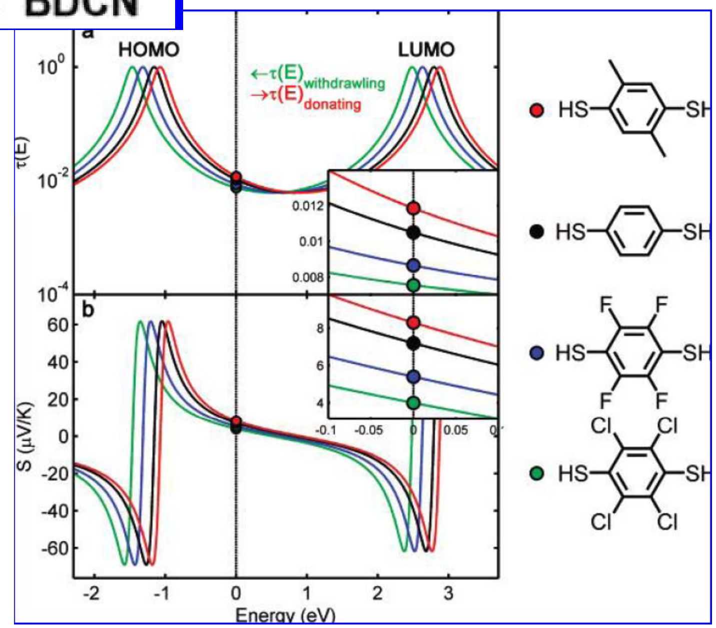

New Ideas

- Combine Phonon-Blocking, Electron-Transmitting Structures Along Heat Flow with Orthogonal Quantum-Confinement for ZT in the range of 4 to 5?

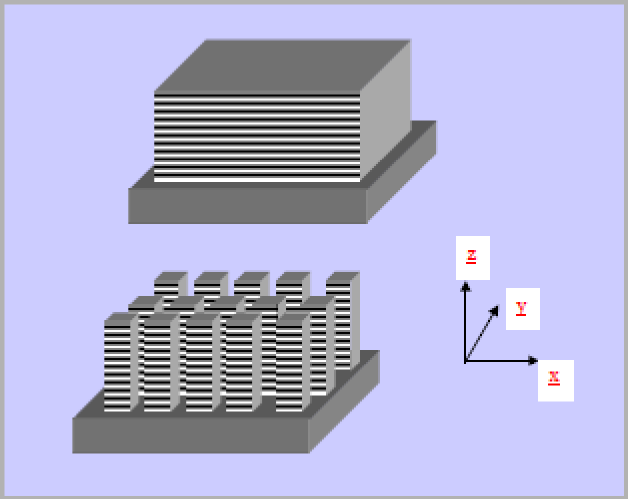

Layered SL Patterned to form 1-di Quantum-Wires – **Orthogonal Quantum Confinement**

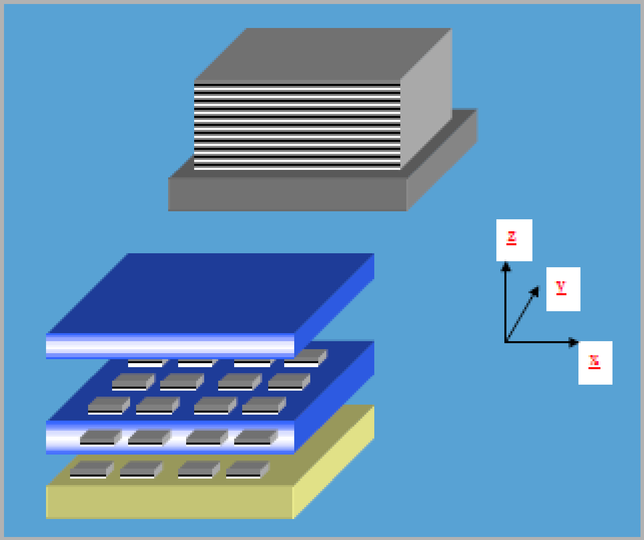

Layered SL Patterned to form Quantum-Boxes – **Orthogonal Quantum Confinement**

Si Nanowires as an Efficient TE Material

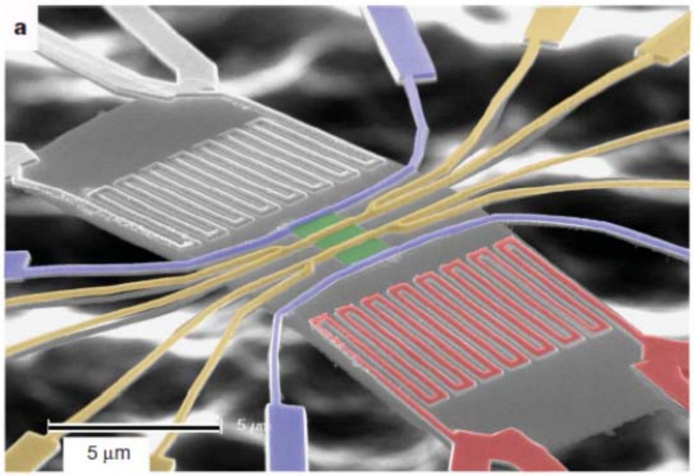

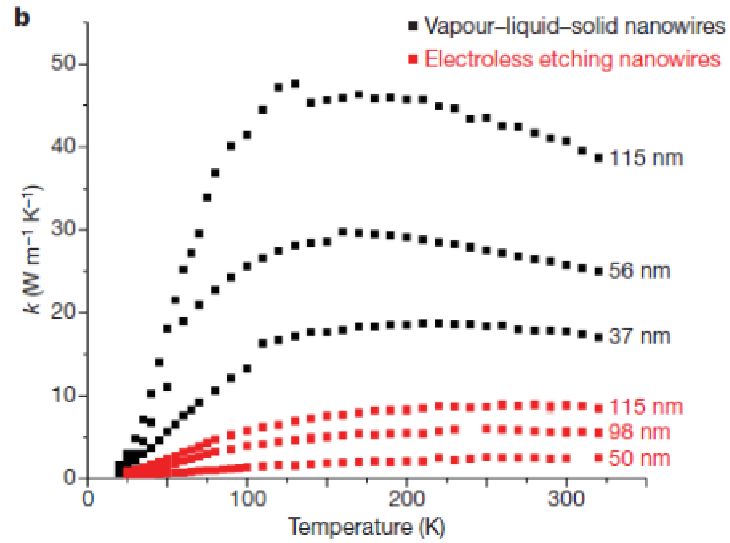

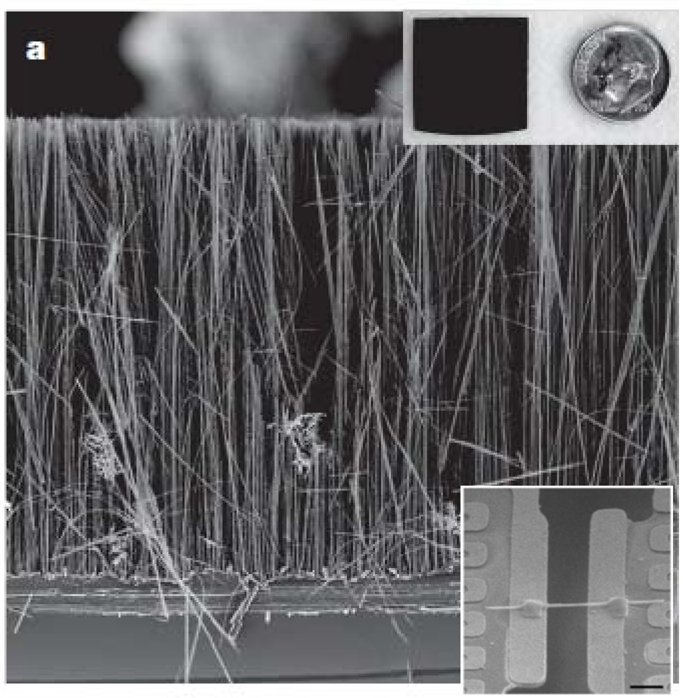

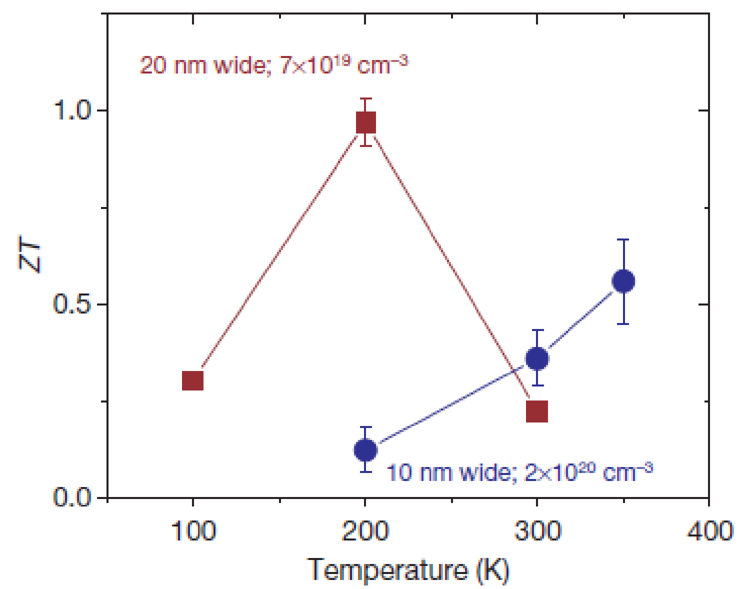

Akram I. Boukai *et al*, Nature **451** 168(2007)

Vol 451|10 January 2008|doi:10.1038/nature06381 nature

Enhanced thermoelectric performance of rough silicon nanowires

Allon I. Hochbaum[1]*, Renkun Chen[2]*, Raul Diaz Delgado[1], Wenjie Liang[1], Erik C. Garnett[1], Mark Najarian[3], Arun Majumdar[2,3,4] & Peidong Yang[1,3,4]

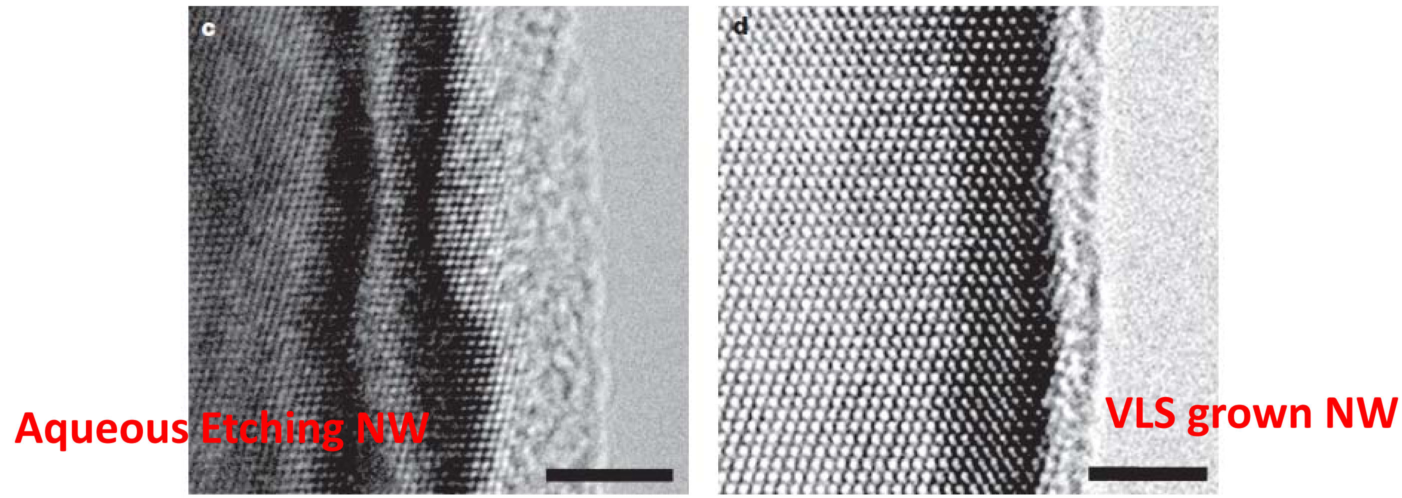

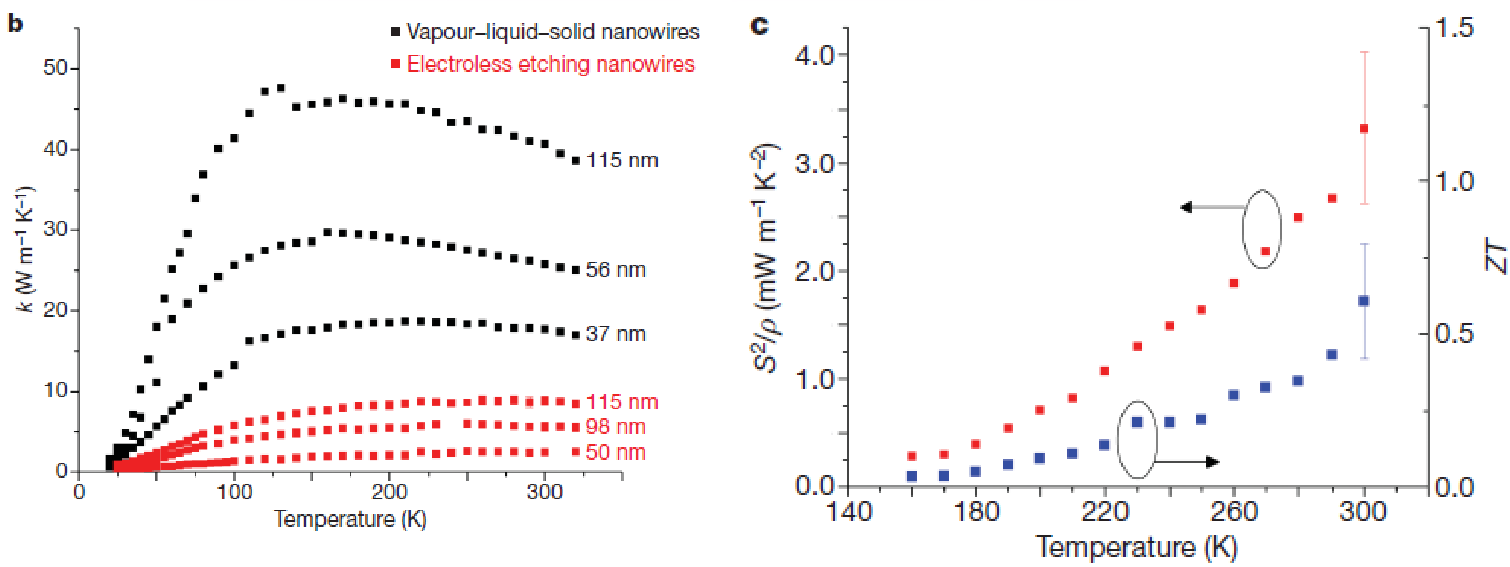

NANO LETTERS

pubs.acs.org/NanoLett

Holey Silicon as an Efficient Thermoelectric Material

Jinyao Tang,[†,§,⊥] Hung-Ta Wang,[†,⊥] Dong Hyun Lee,[‖] Melissa Fardy,[†] Ziyang Huo,[†] Thomas P. Russell,[‖] and Peidong Yang*[,†,‡,§]

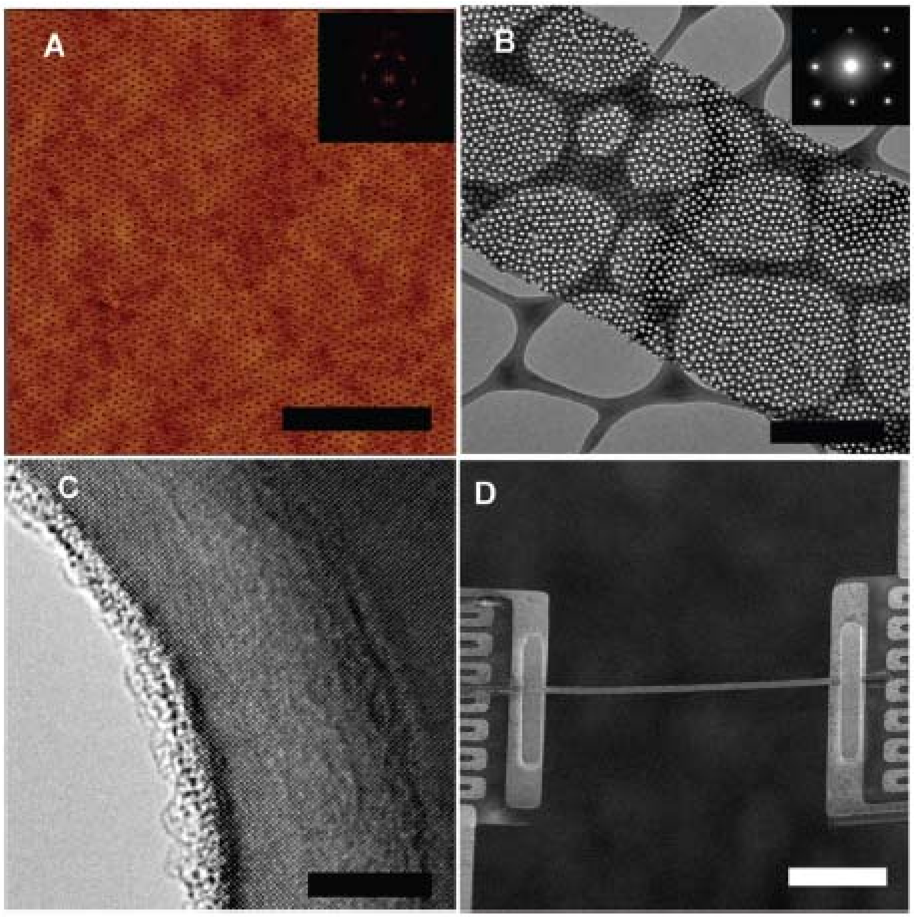

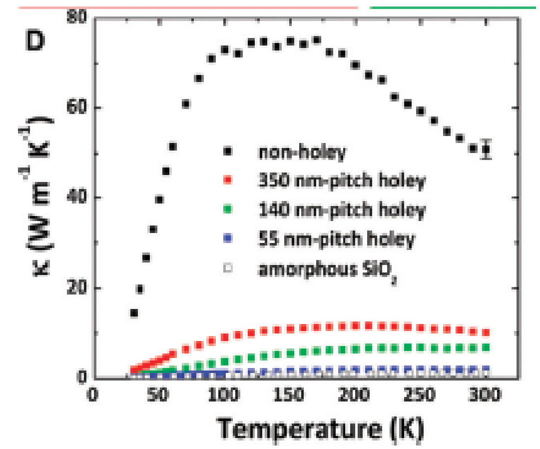

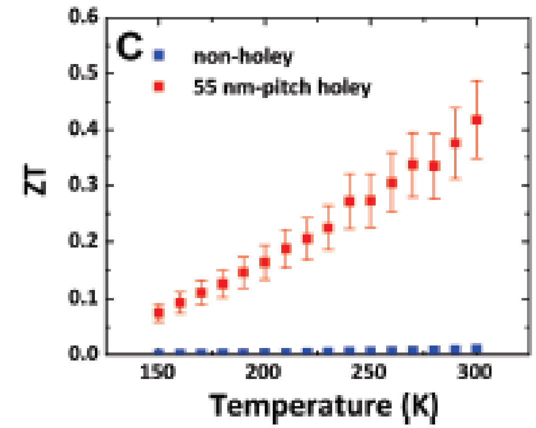

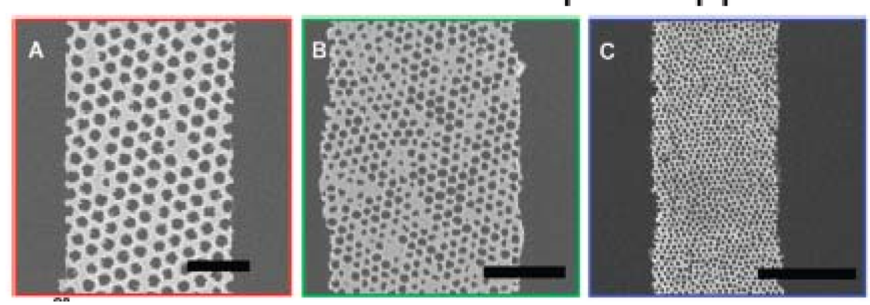

TABLE 1. Summary of the HS Geometry and the Thermal Conductivity at 300 K[a]

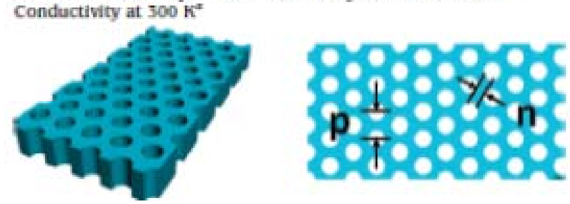

Nano-composite & Nanowires

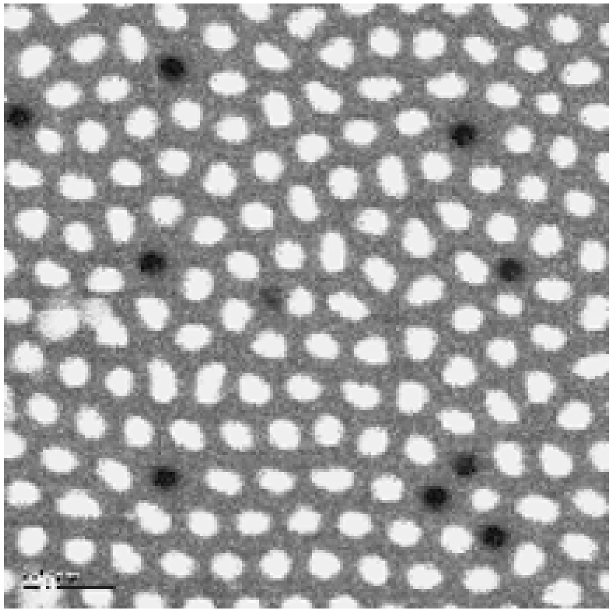

Nano-composite

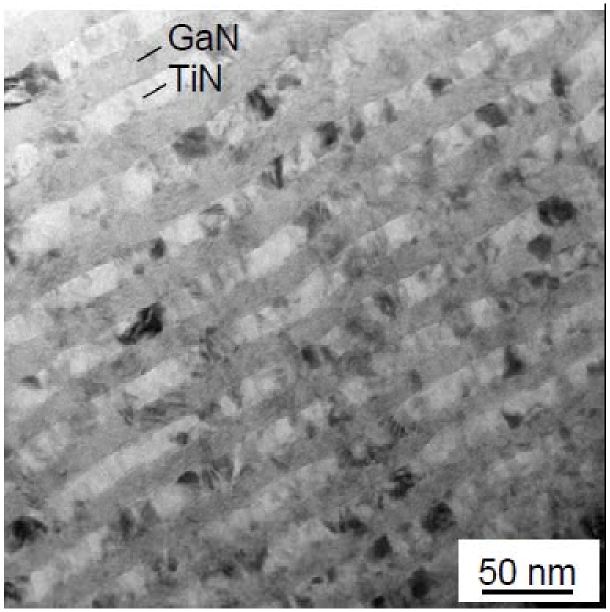

Super-lattice structure

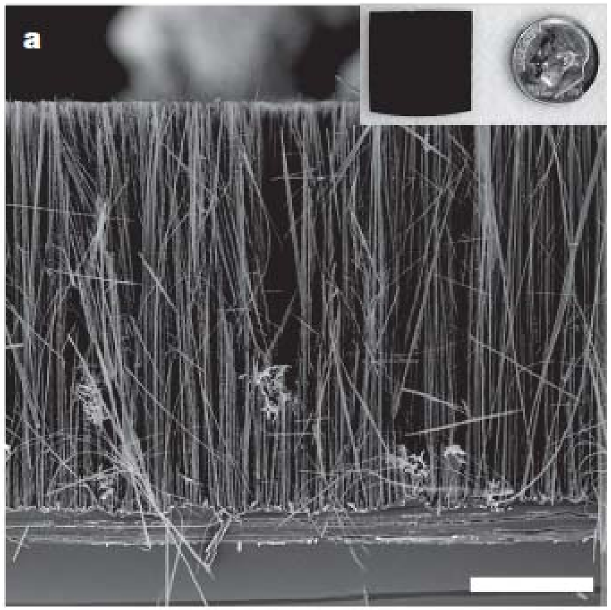

Nanowires

Goal: Reduce Thermal conductivity or Increase electrical conductivity

T. Sands et al, Purdue University
Akram I. Boukai *et al*, Nature **451** 168(2007)

Lamellae of Thermoelectric PbTe and Sb_2Te_3

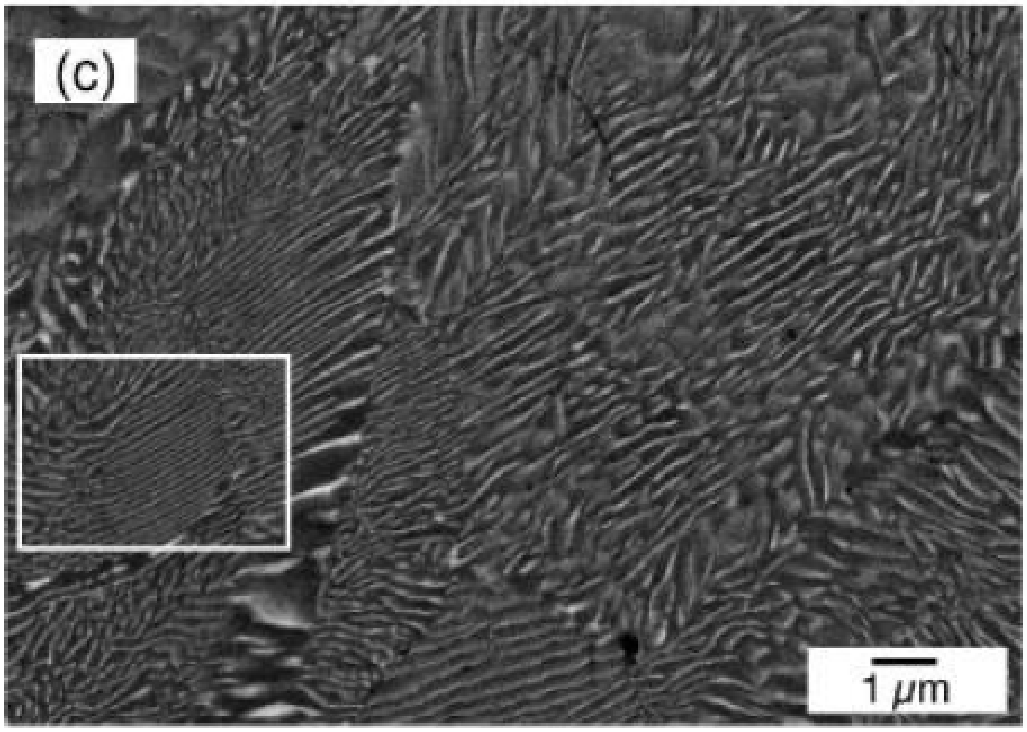

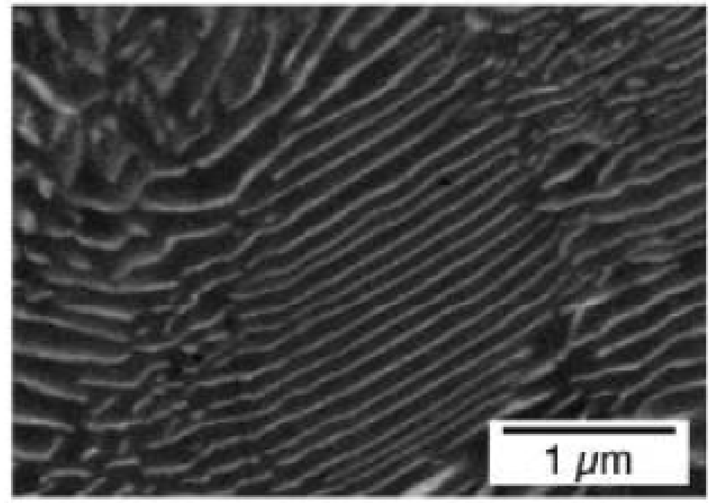

Jeffrey Snyder *Chem. Mater., Vol. 19, No. 4, 2007* 765

ZT of $Si_{0.8}Ge_{0.2}B_{0.016}$ by ball milling

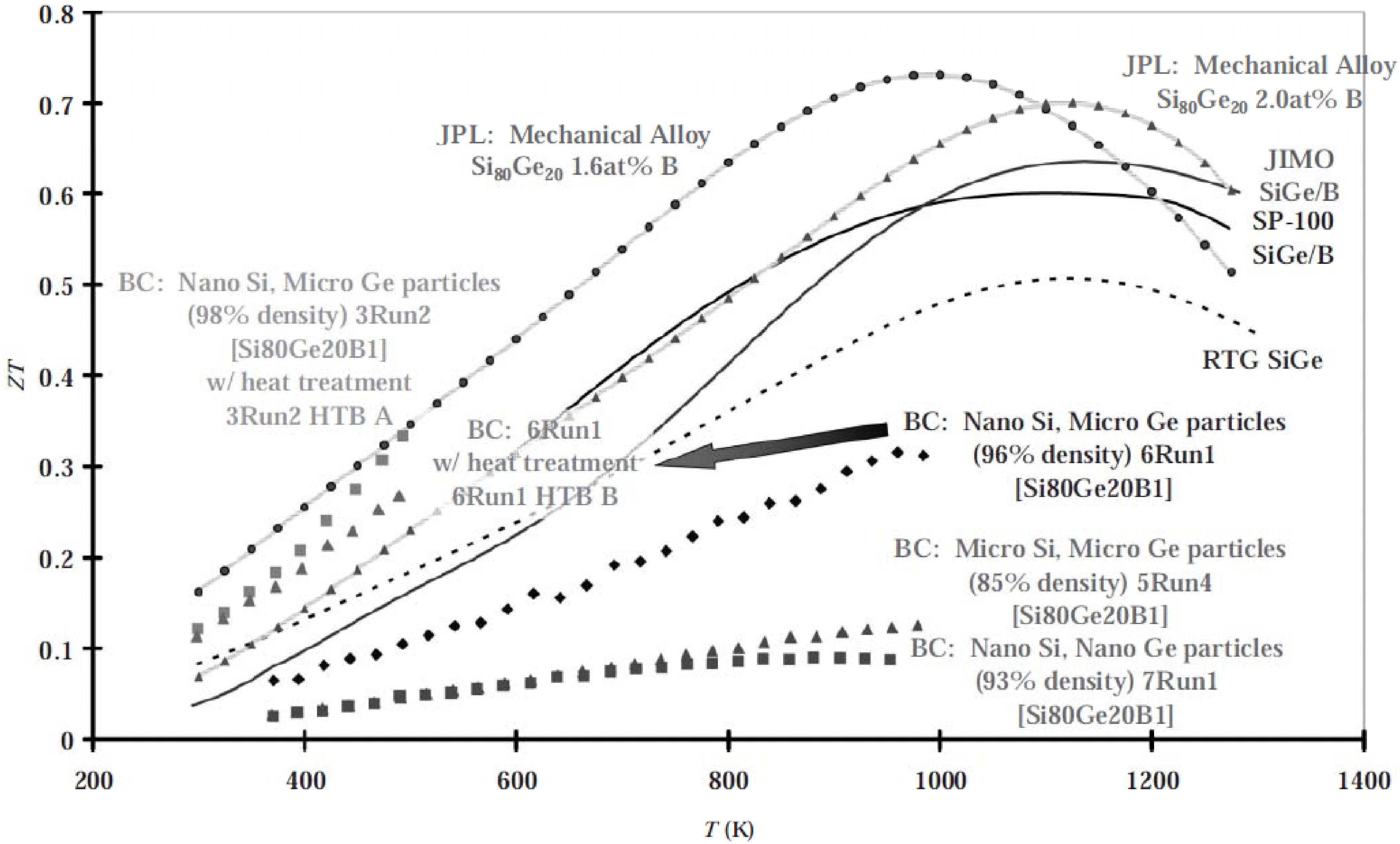

Adv. Mater. **2007**, *19*, 1043–1053

1-D Nano Materials in AML

JACS 123, 2791 (2001)
APL 81, 22 (2002)
JACS 127, 2820 (2005)
APL 90, 213104 (2007)
Adv. Func. Mater. (2008)
Small 4, 925 (2008)
Electrochem. Comm. 11, 850 (2009)
Anal. Chem. 81, 36 (2009)
Angew. Chem. Int. Ed. 49, 5966 (2010)

Wire/Rod

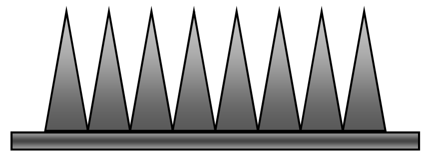

Nanotip

APL 83, 1420 (2003)
Nano. Lett. 4, 471 (2004)
Chem. Mater. 17, 553 (2005)
Adv. Func. Mater. 15, 783 (2005)
APL 86, 203119 (2005)
US Patent 6,960,528,B2
APL 89, 143105 (2006)
Nature Nanotech. 2, 170 (2007)
Nano Lett. 9, 1938 (2009)

APL 81, 4189 (2002)
Adv. Func. Mater. 12, 687 (2002)
APL 86, 203119 (2005)
JACS 128, 8368 (2006)
PRB 75, 195429 (2007)
J. Power Sources 171, 55 (2007)
JACS 130, 3543 (2008)
J. Power Sources 190, 279 (2009)

Tube

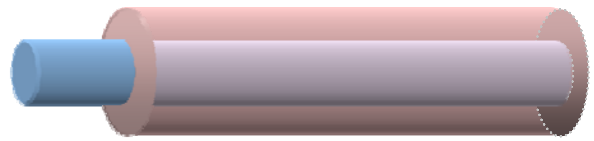

Core-shell

APL 81, 1312 (2002)
Nano. Lett. 3, 537 (2003)

Chapter 9, pp. 259-309, Nanowires and nanobelts, Kluwer (2004)
Adv. Func. Mater. 16, 537 (2006)
APL 90, 123109 (2007)
Adv. Mater. 19, 4524 (2007)
Opt. Express 17, 11690 (2009)

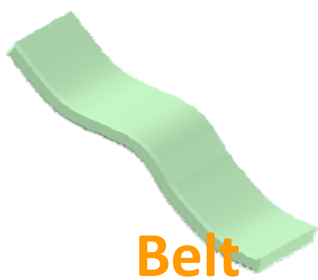

Belt

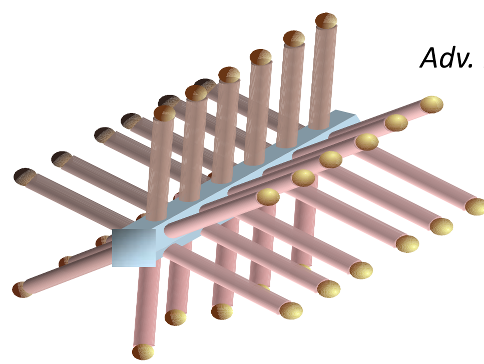

Brush

Adv. Func. Mater. 14, 233 (2004)

Other related:
APL 86, 21911 (2005)
APL 86, 83104 (2005)
APL 86, 161901 (2005)
APL 87, 261915 (2005)
JVST B 24, 87 (2006)
APL 88, 73515 (2006)
Adv. Mater. 21, 259 (2009)
Angew. Chem. 48,7586 (2009)
J. Mater. Chem. (2010)

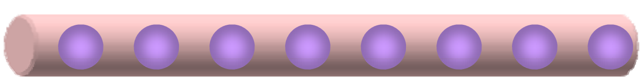

Peapod

Adv. Mater. 14, 1847 (2002)
Nature Mater. 5, 102 (2006)

Applications: Solar Harvesting

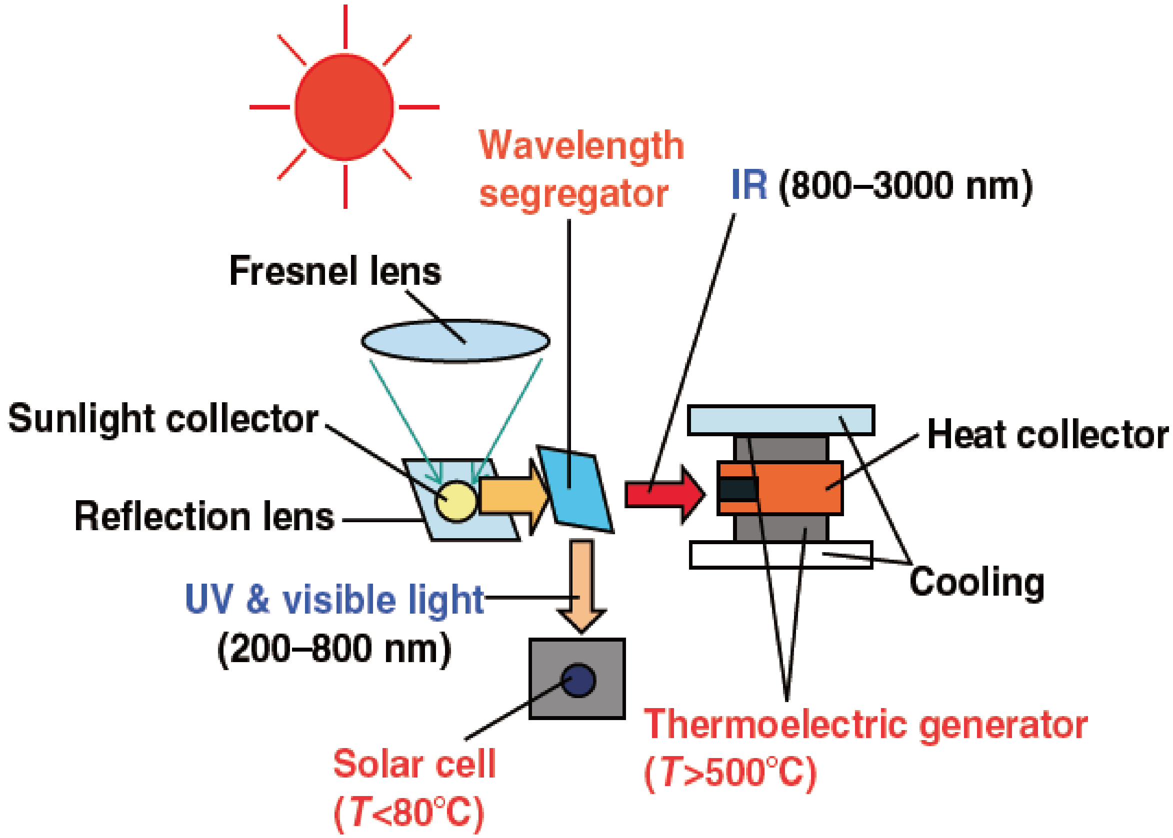

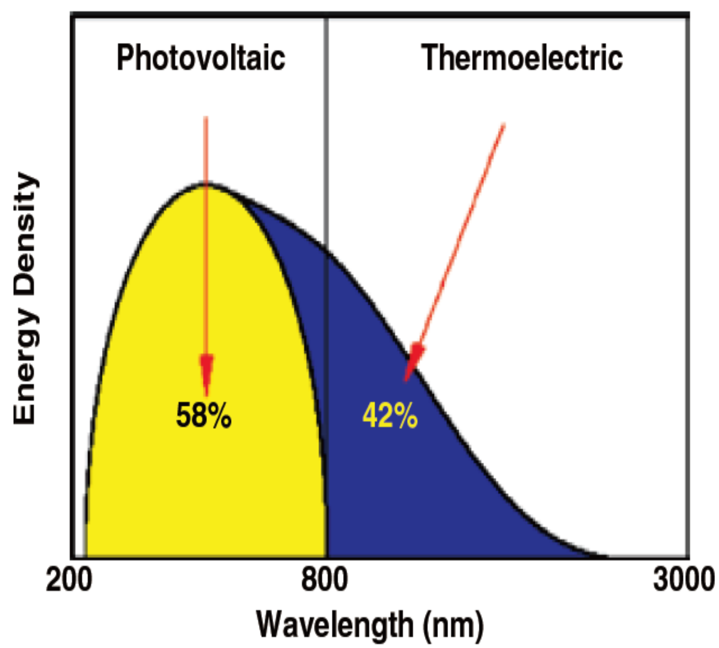

Nanocomposites

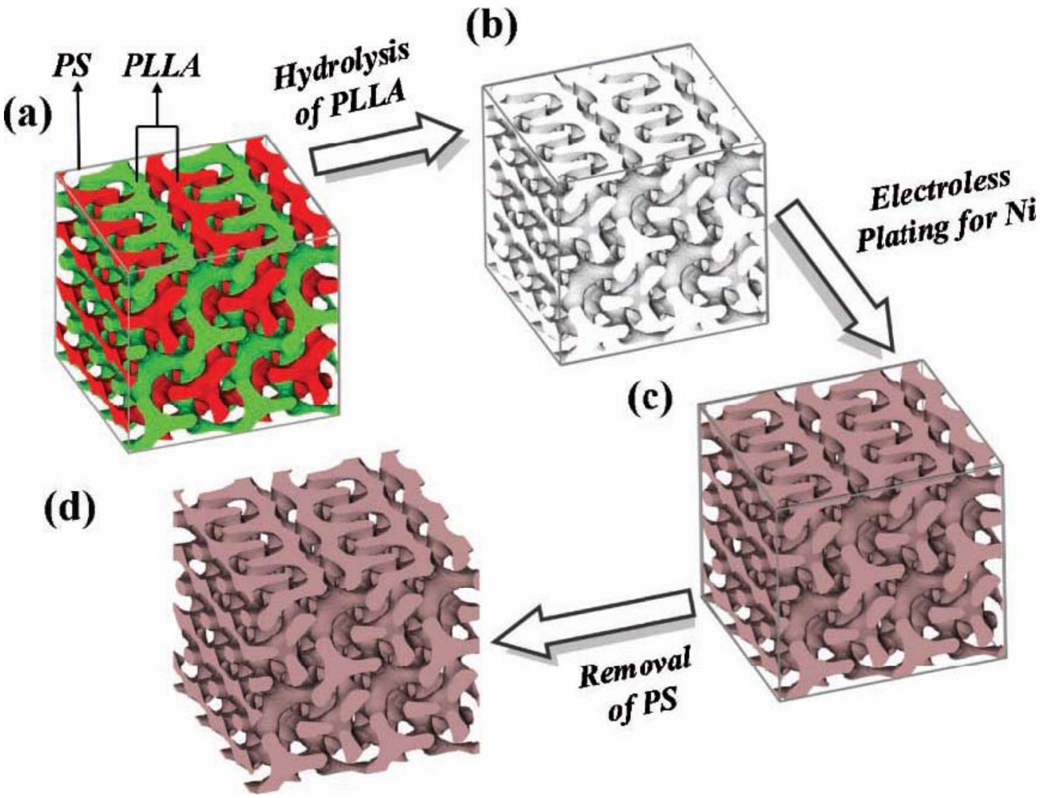

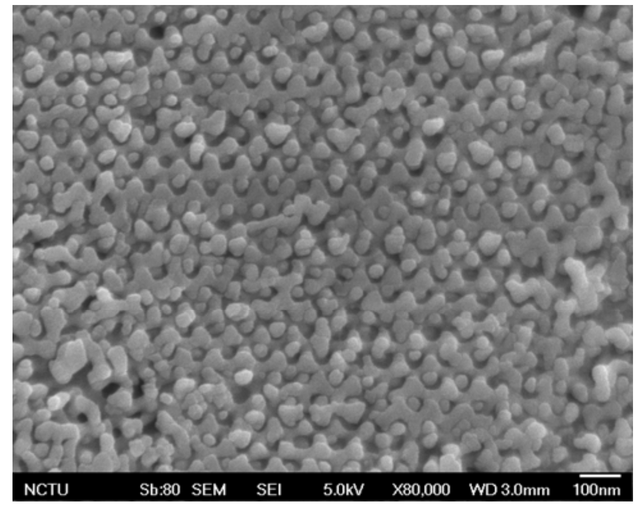

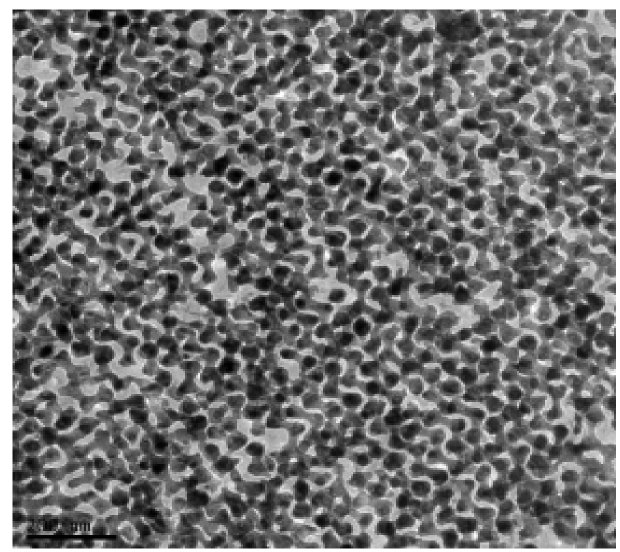

TE Measurement

Multiwall carbon nanotube

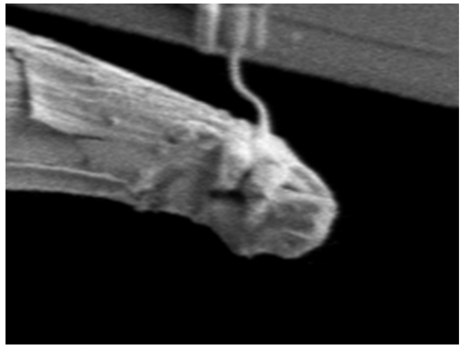

Silver nanowire

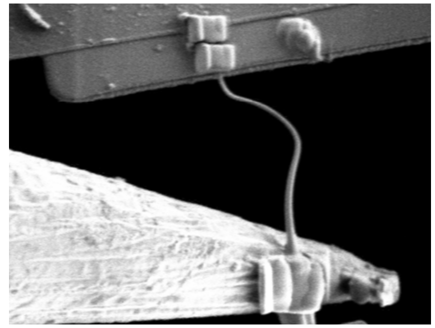

ZnO nanowire

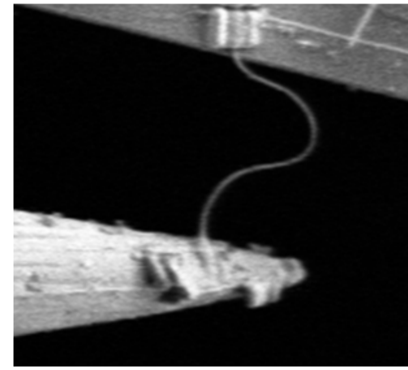

Ga_2O_3 nanowire

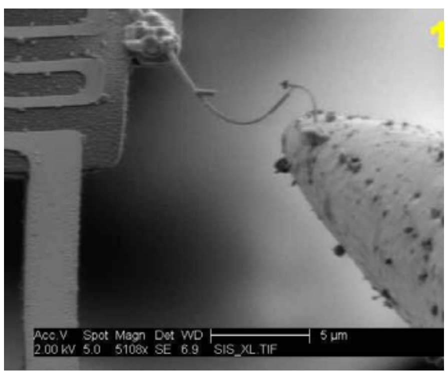

Undoped Si nanowire

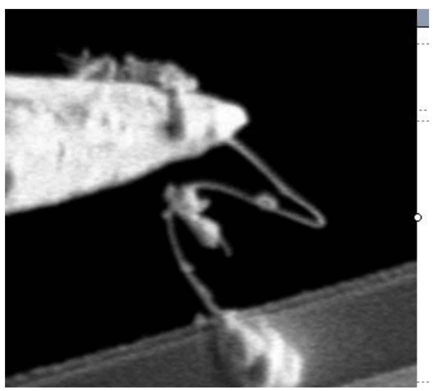

P-type Si nanowire

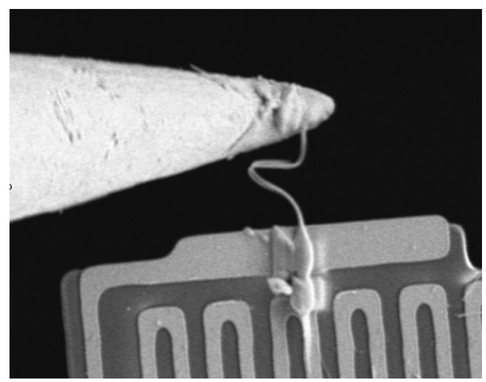

N-type Si nanowire

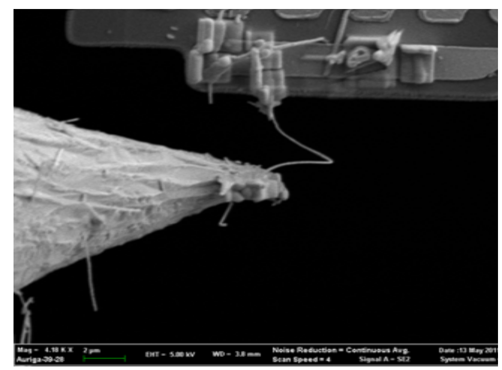

SiGe nanowire

Thermal conductivities remain intact under extreme strain

SWCNT goes beyond the theoretical limit of 1D ballistic phonon transport

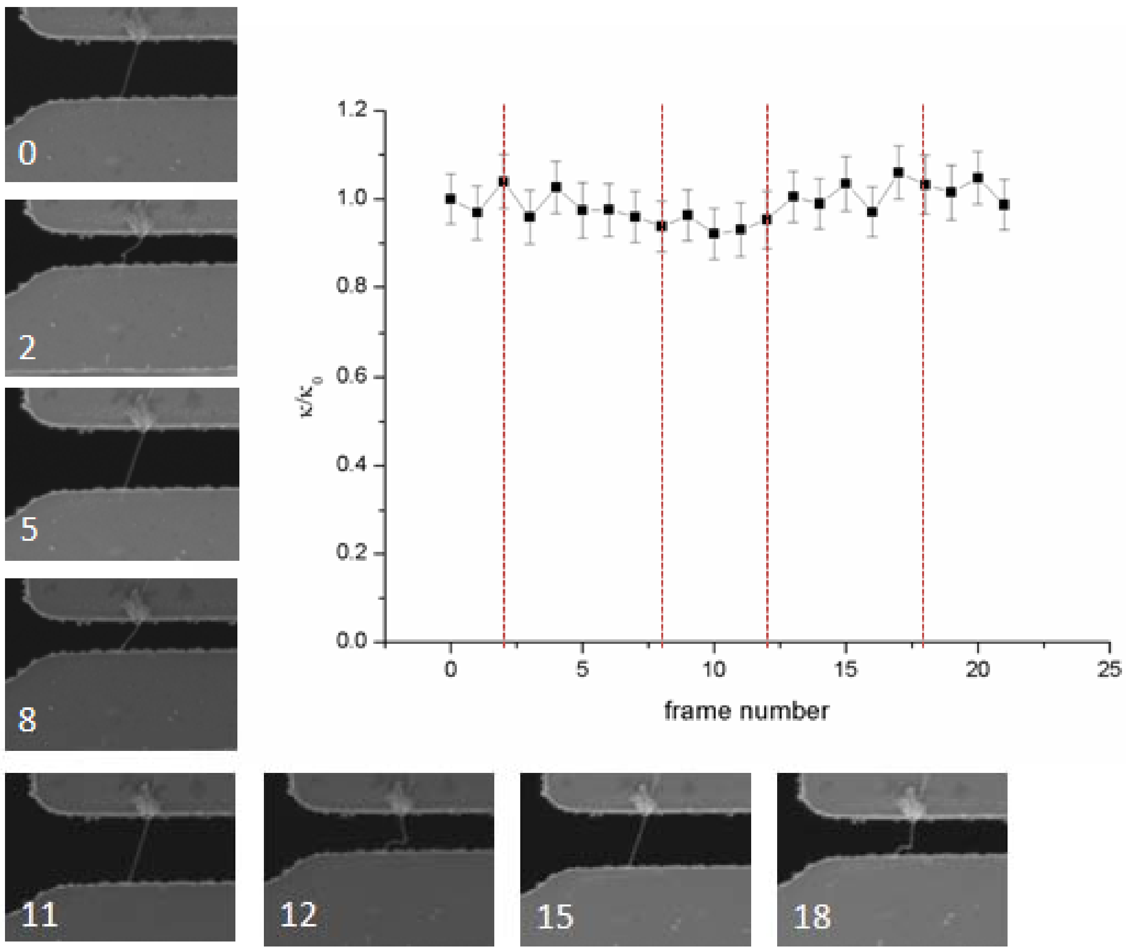

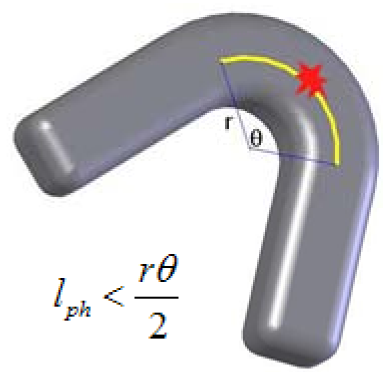

No changes of thermal conductivity is observed even when the bending radius of curvature is less than the phonon mean free path.

Modulation of ZT by Strain
(Possible active TE device!)

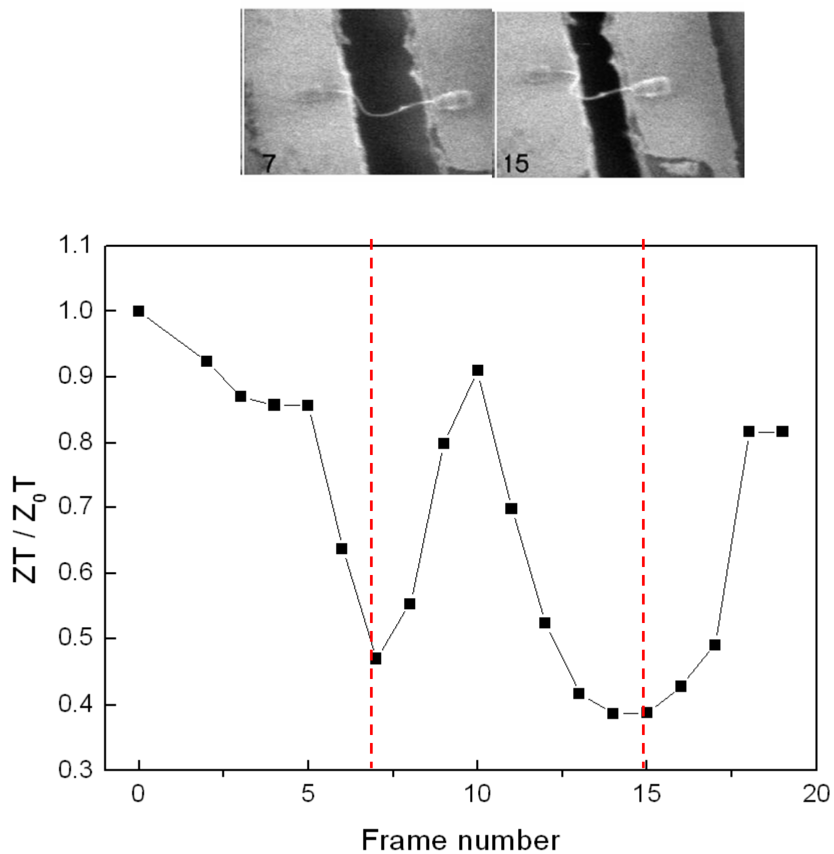

Carbon nanotube

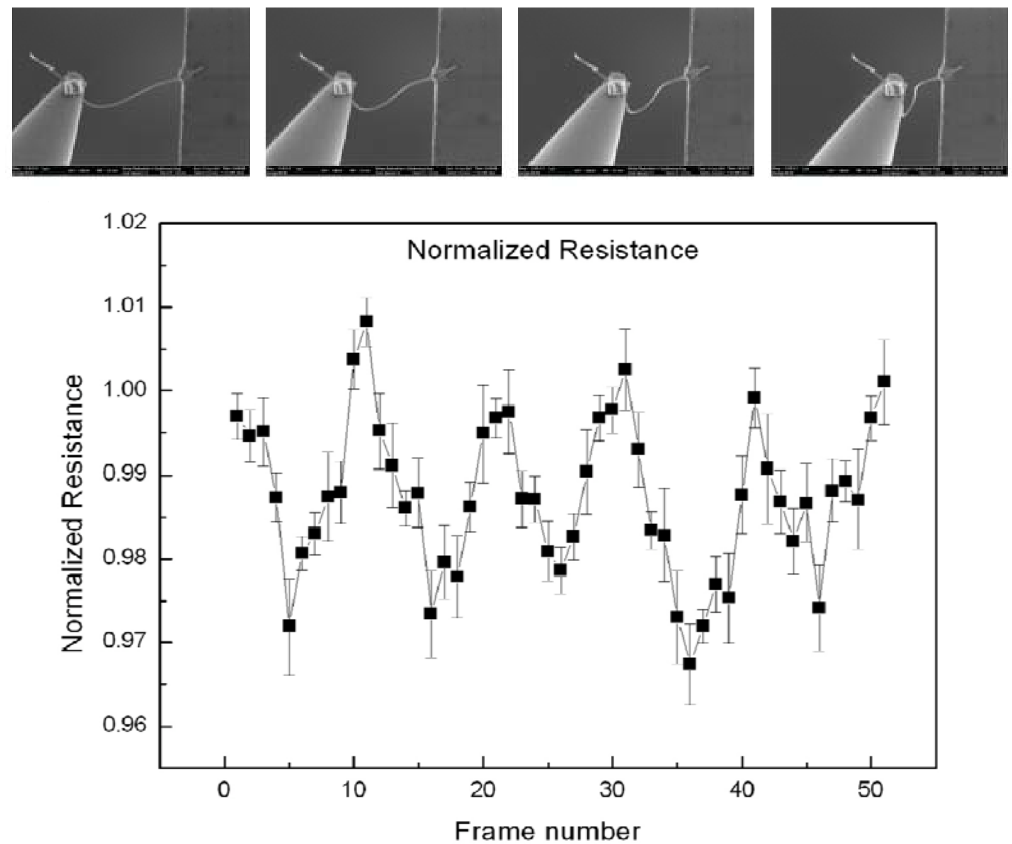

Silicon nanowire (p-type)

Thermopower responses are currently under investigation.

Crystal Structure of Bi_2Se_3

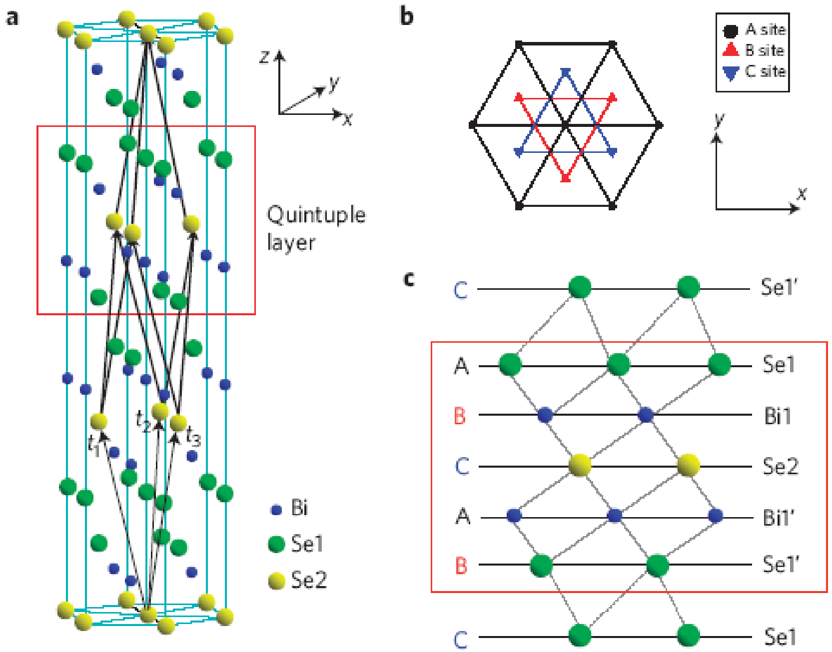

Crystal structure of Bi_2Se_3

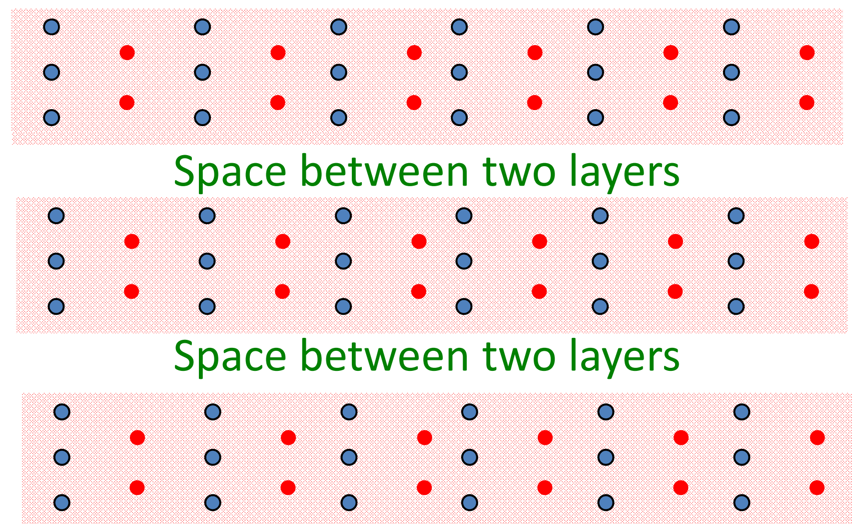

Bi_2Se_3 cleaves easily along the trigonal axis due to van der Waals bonding between neighboring selenium layers.

Haijun Zhang *et al*, Nature materials **5** 438 (2009)

F. C. Chou's lab

Graphene-Intercalation in Bi_2Se_3

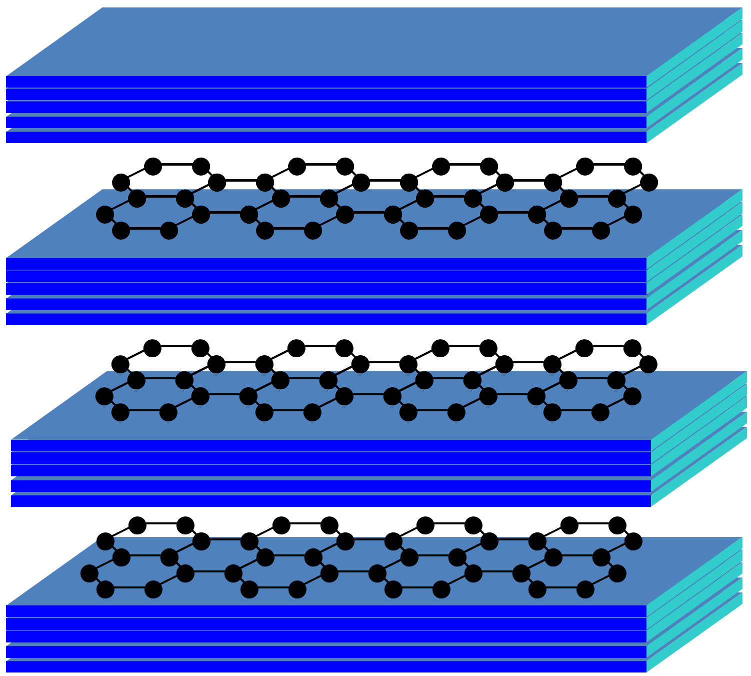

Bi_2Te_3

One or few layer graphite

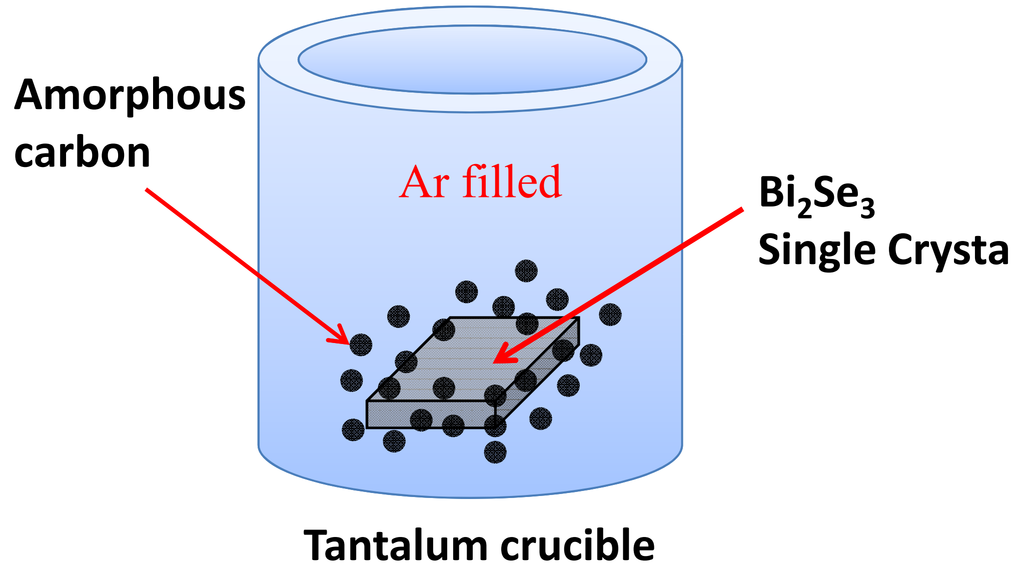

Annealed under ~2 atm, 400°C, 2 weeks.

Bi_2Se_3 crystal well packed with carbon

Bi_2Se_3	G-intercalated Bi_2Se_3
Soft	**Brittle**

XRD Pattern of Bi_2Se_3 Single Crystal

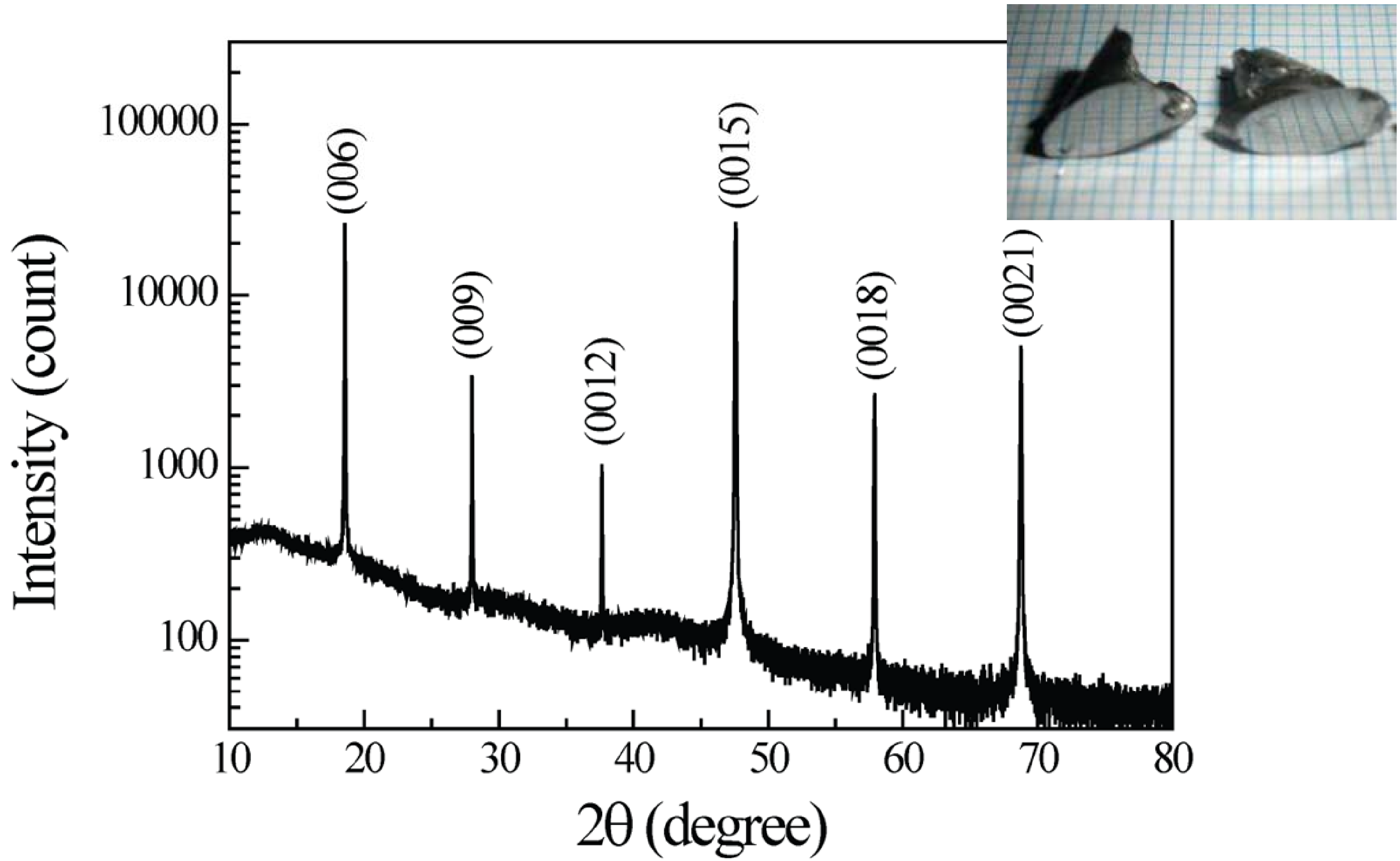

XRD pattern of pure Bi_2Se_3 depicts it superior crystal quality.

XRD Pattern of Bi_2Se_3 After Intercalation

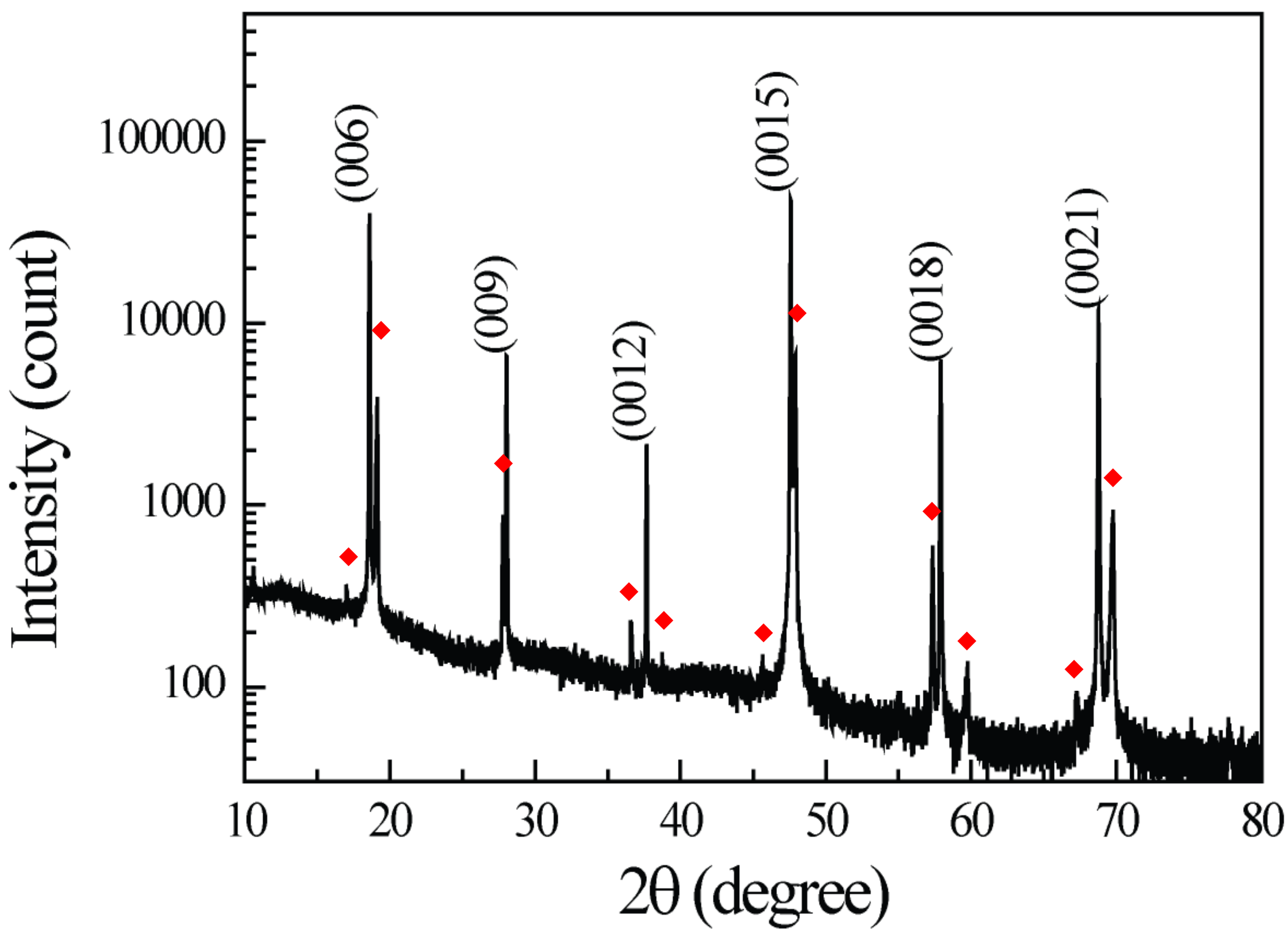

XRD pattern of Bi2Se3 with carbon intercalated.
Unknown peaks near main peaks can be observed.

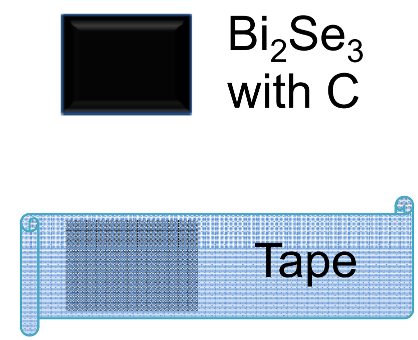

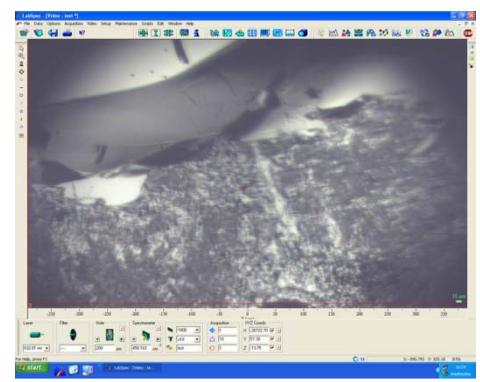

The Bi_2Se_3 layer can be flaked off from the crystal.

Raman Spectrum of Bi_2Se_3 with G-Intercalation

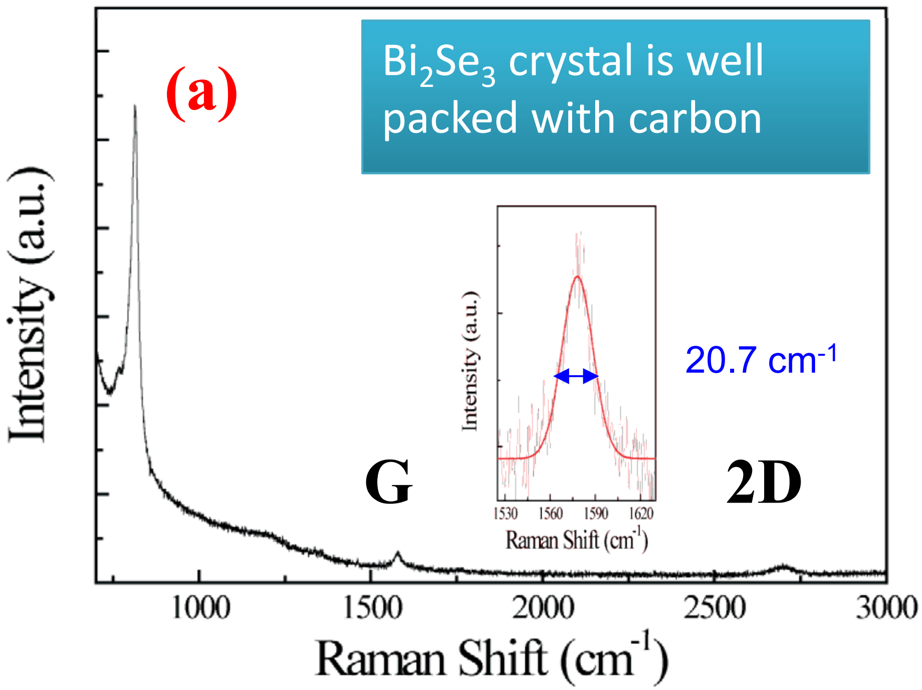

The Raman spectrum of carbon-intercalated Bi_2Se_3. Amorphous carbon diffused into crystal and formed graphite-like structure.

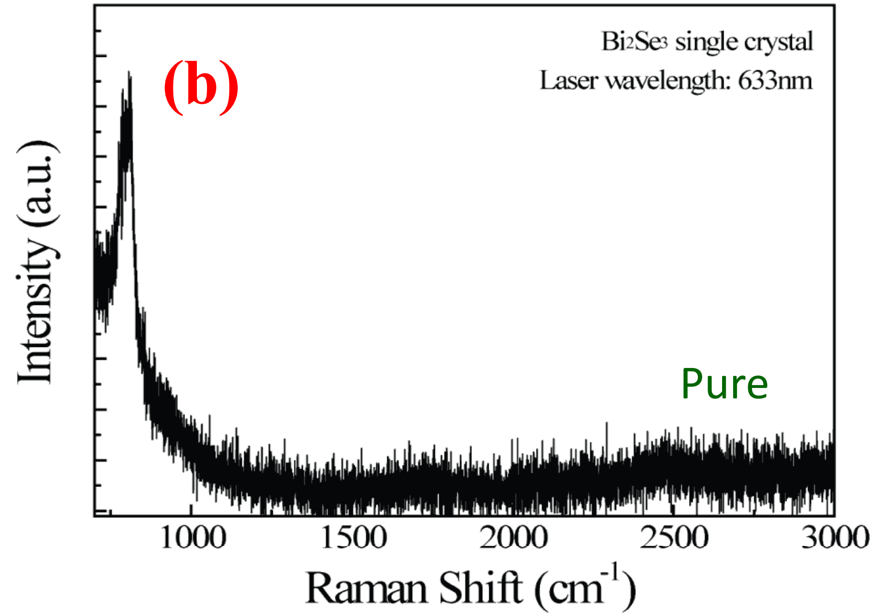

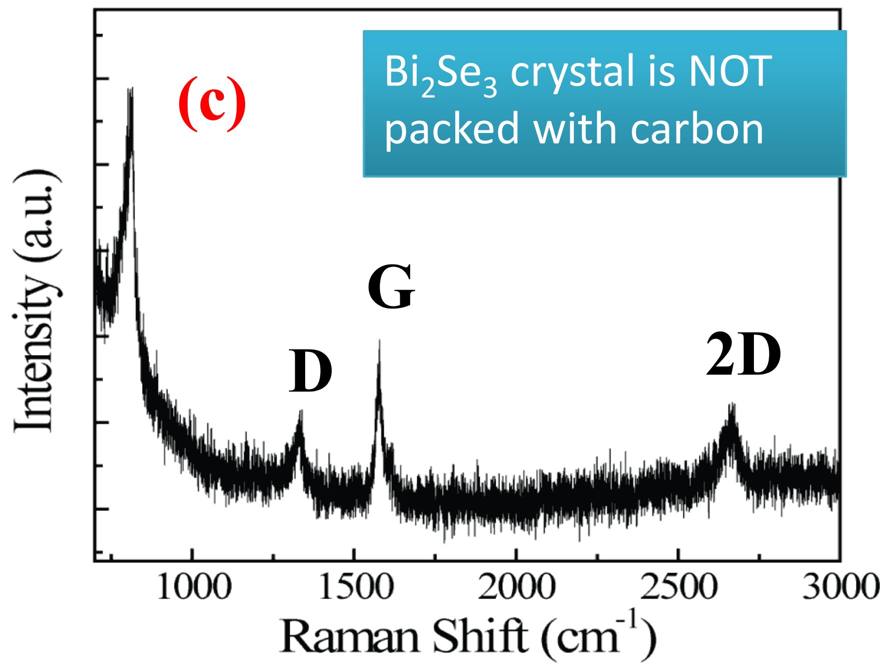

TE Technique: Seebeck Coefficient & Electrical Conductivity

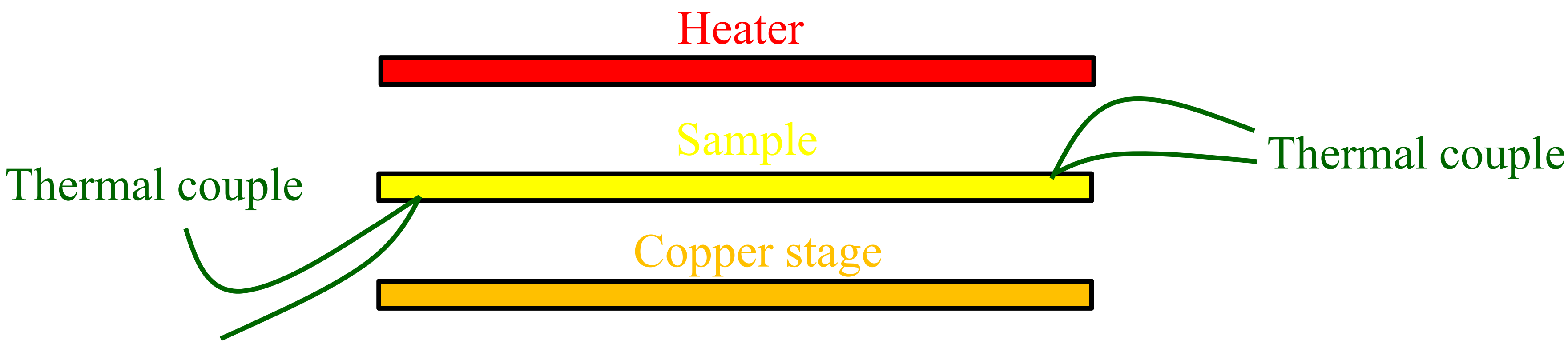

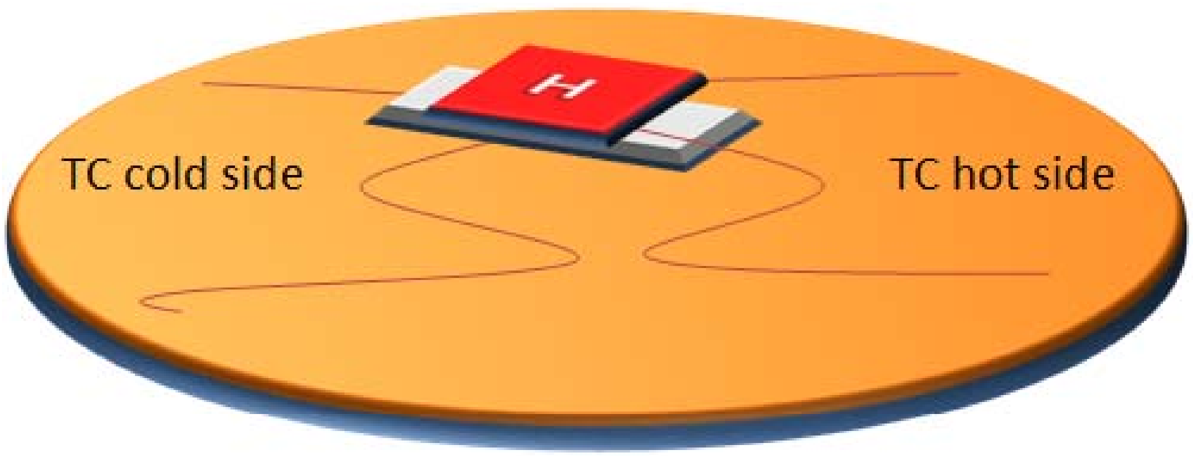

Thermal Diffusivity Measurement

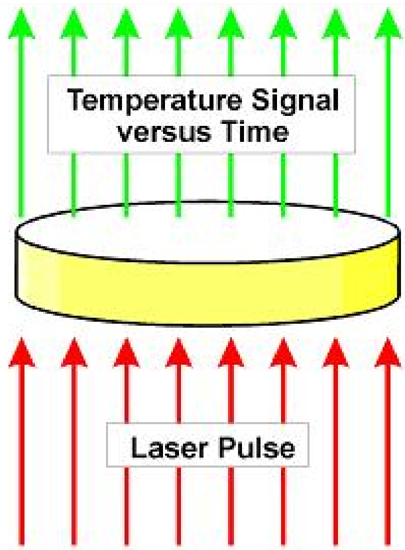

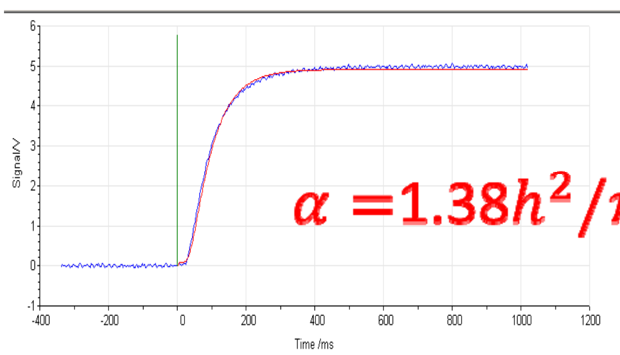

$$\alpha = 1.38h^2/\pi^2 t_{0.5}$$

We can get the thermal diffusivity by measure the "half-time" of temperature increase resulted from laser heating.

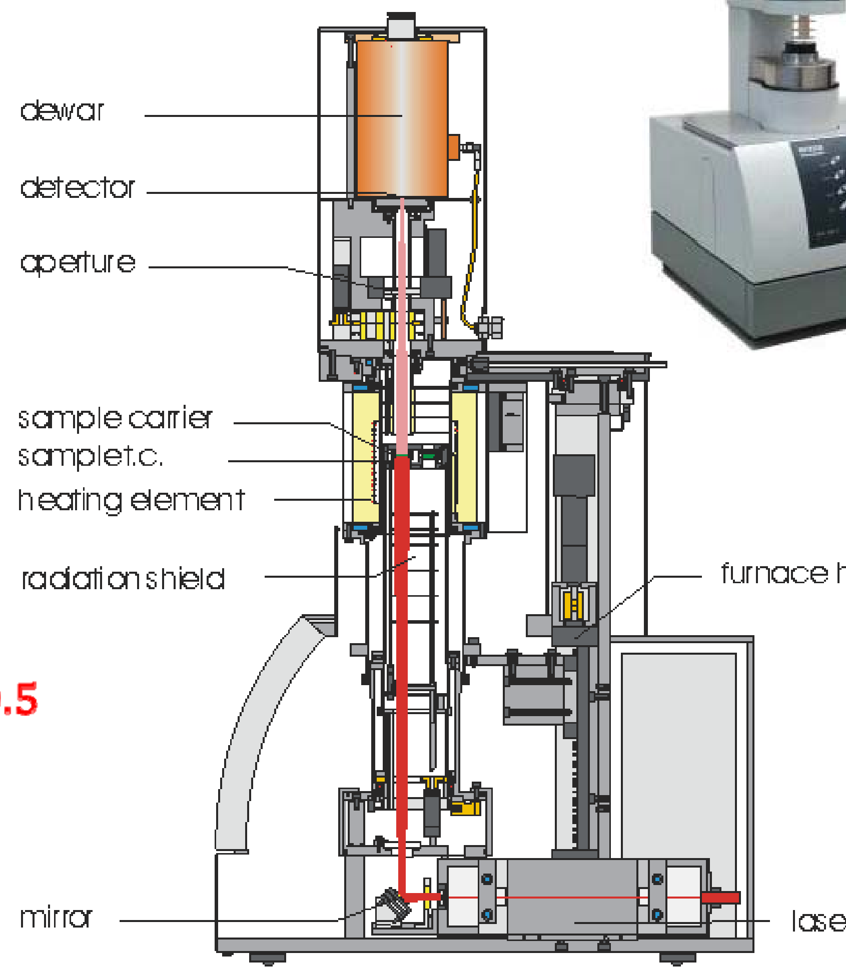

Cooperator: Dr. Y. Chen's lab

Reduction of Thermal Conductivity in Nanowires

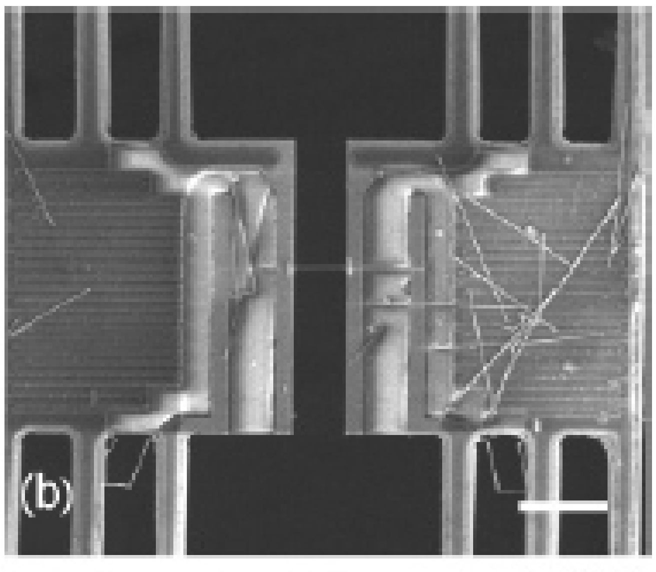

The Seebeck coefficient, electrical conductivity, and thermal conductivity, can be measured via using the micro-thermometer device.
(Cooperator: Chih-Wei Chang)

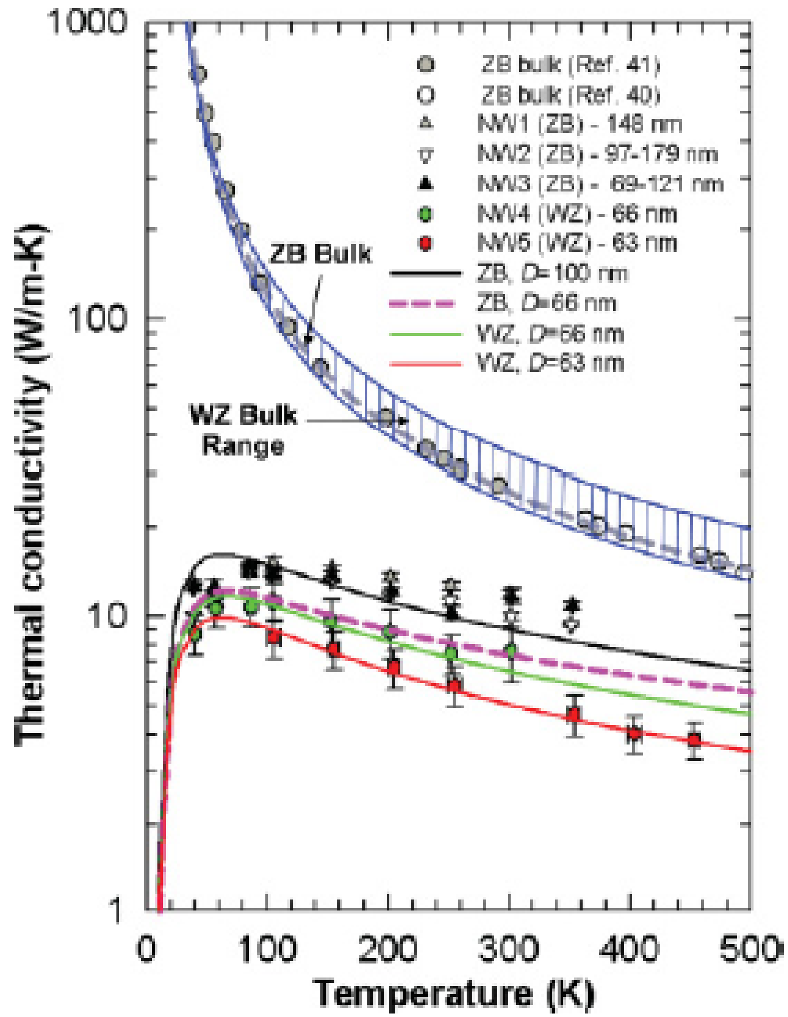

Thermal conductivities of InAs nanowires with different diameters.

Feng Zhou et al, PRB 83, 205416 (2011)

Power Factor Enhancement of Nanowires

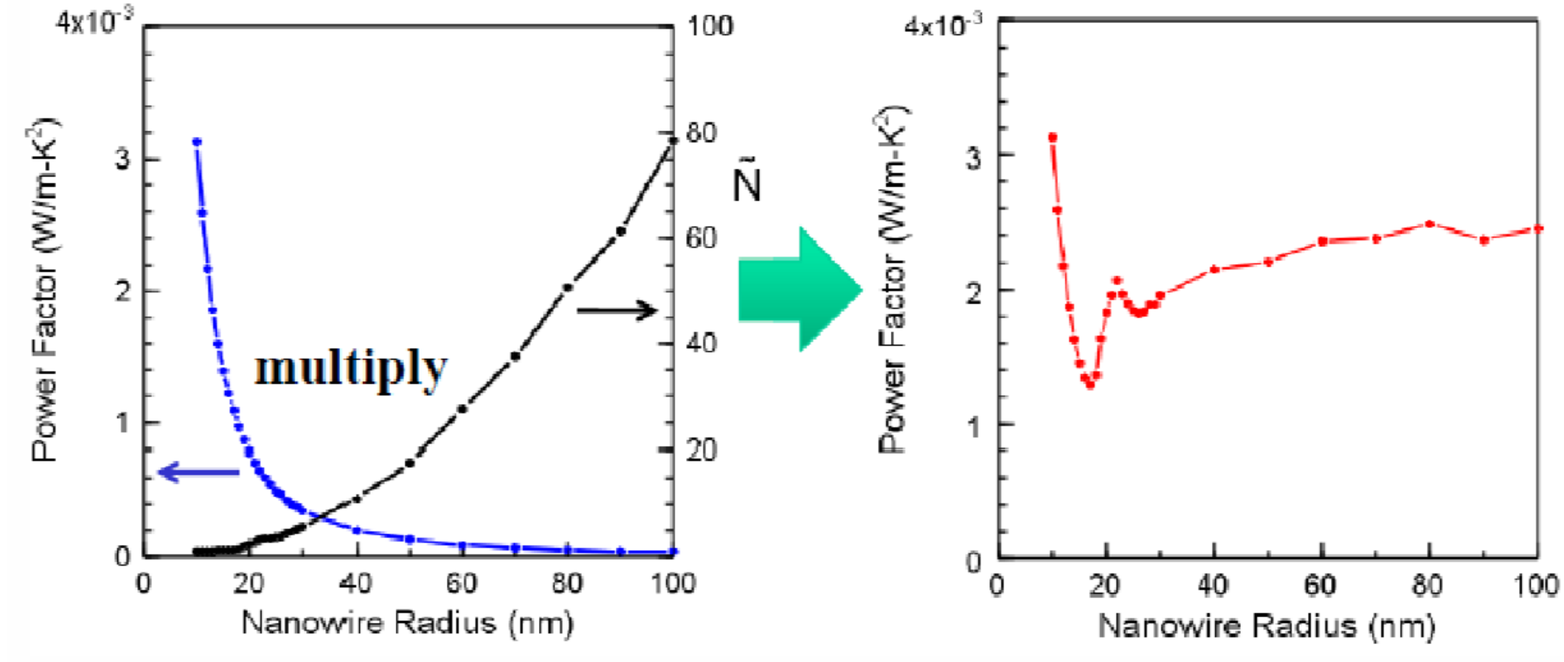

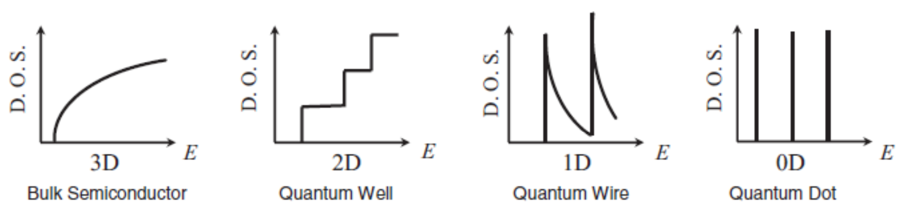

Figure 1. Electronic density of states for a) a bulk 3D crystalline semiconductor, b) a 2D quantum well, c) a 1D nanowire or nanotube, and d) a 0D quantum dot. Materials systems with low dimensionality also exhibit physical phenomena, other than a high density of electronic states (DOS), that may be useful for enhancing thermoelectric performance (see text).

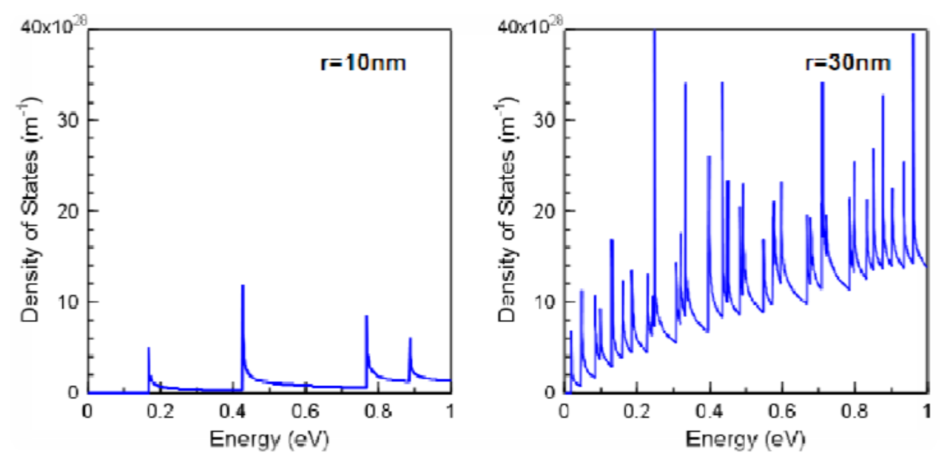

$$PF(r) = PF\,(r)_{one\ subband} \times \text{Numbers of Subbands}(r)$$

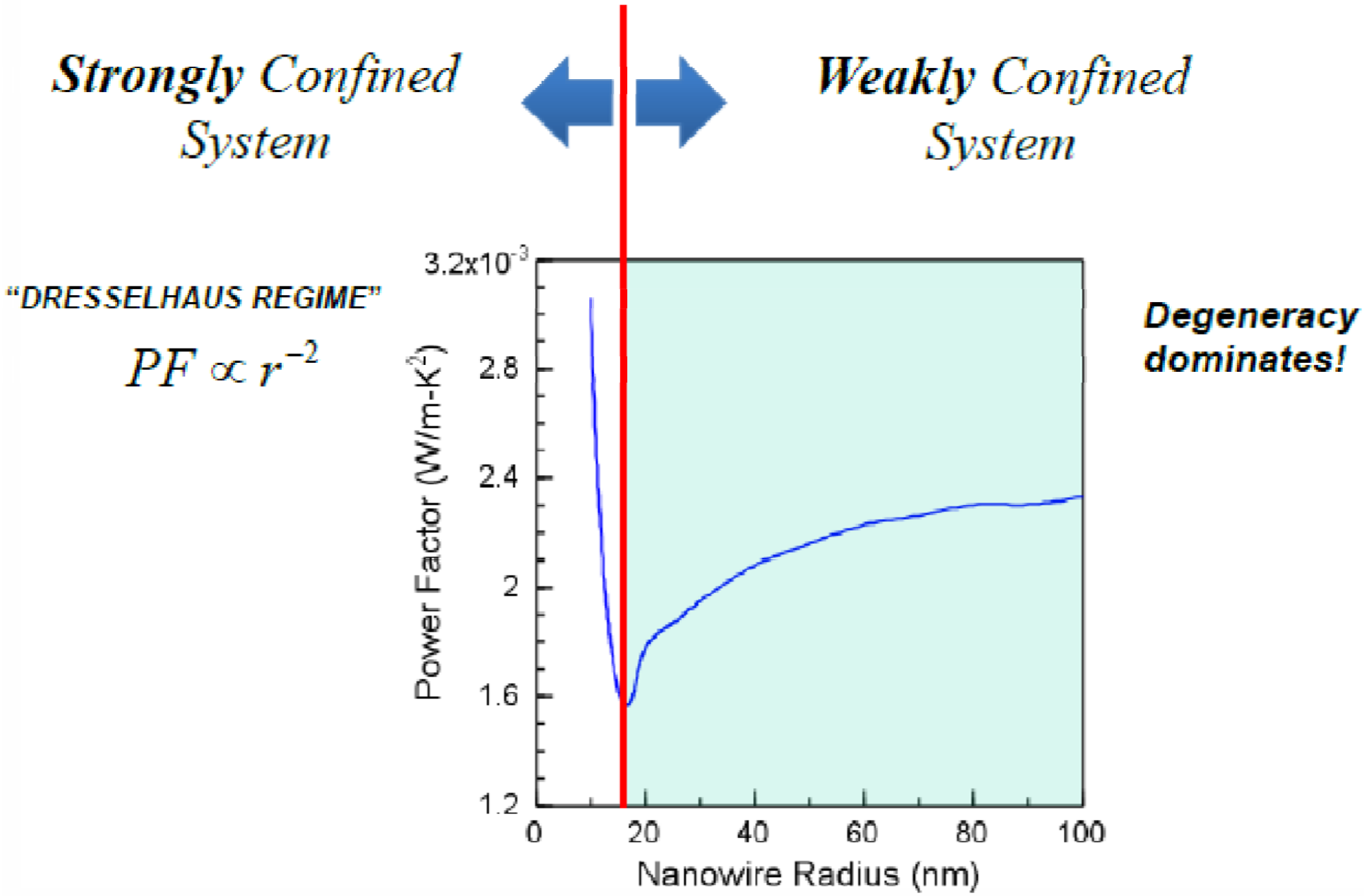

Strongly Confined System
Weakly Confined System
"DRESSELHAUS REGIME"
$PF \propto r^{-2}$
Degeneracy dominates!
3.2x10^{-3}
2.8
2.4
2
1.6
1.2
Power Factor (W/m-K^2)
0
20
40
60
80
100
Nanowire Radius (nm)

Ultra-thin GaN Nanowires grown by MOCVD

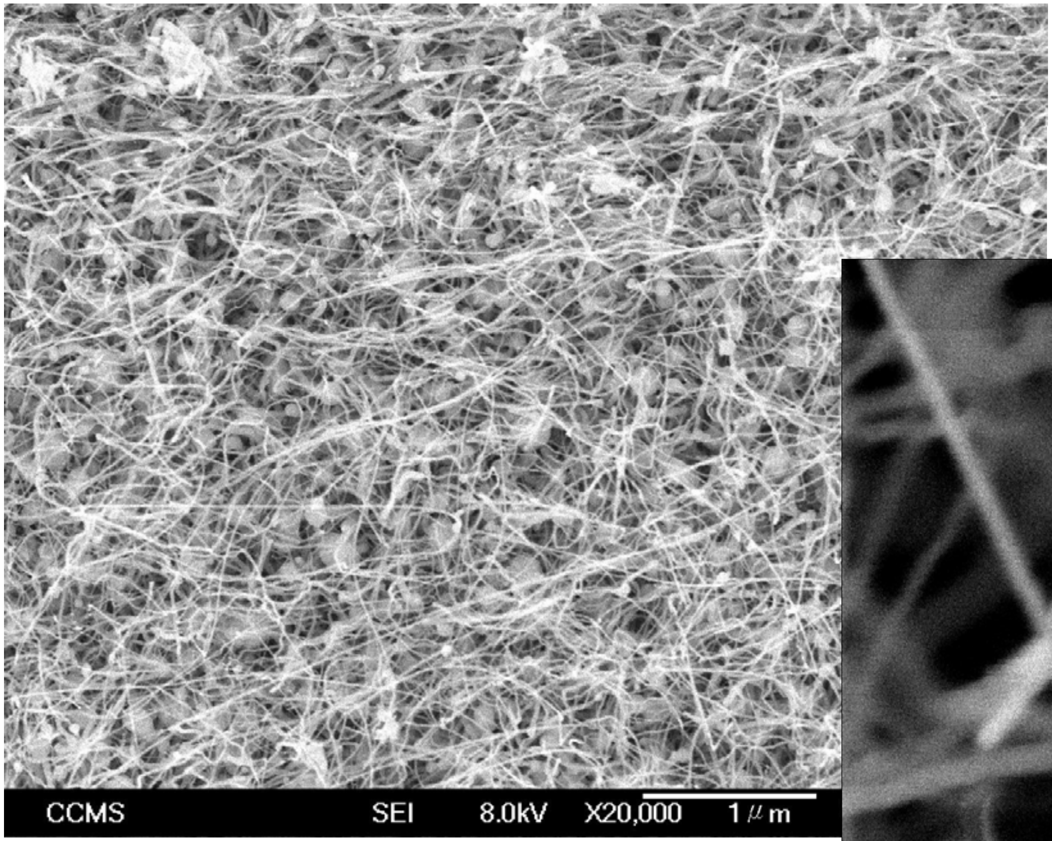

10μm long & 10nm wide GaN NWs!!

Nitride-Based Thermoelectric Materials

AlN GaN InN

AlGaN InGaN

AlInN

Insulator → Conductor

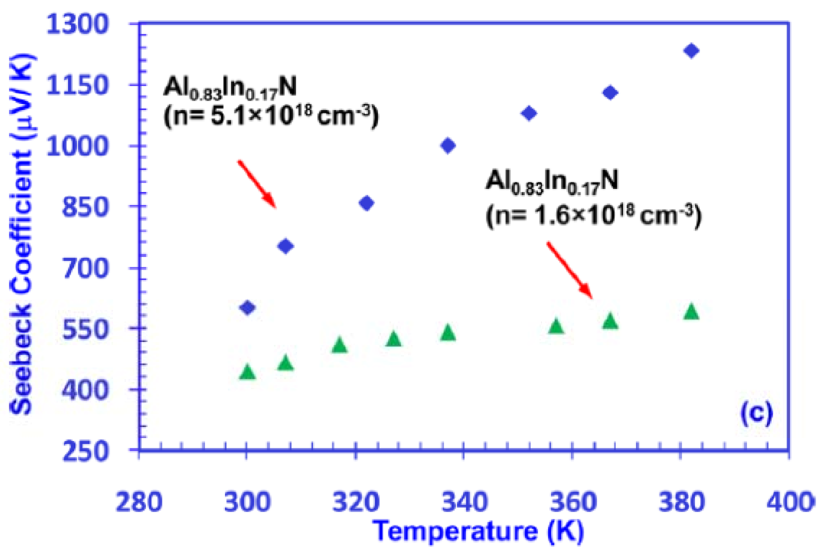

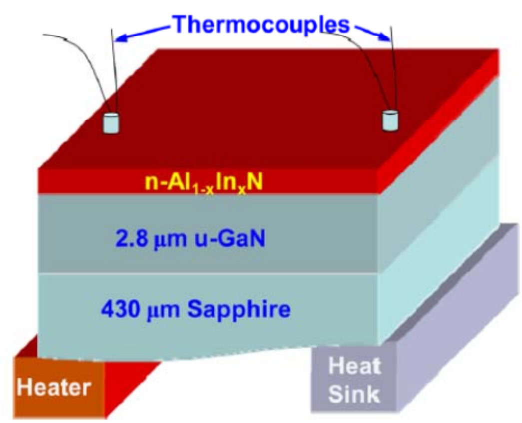

III-Nitride groups are expected to be good TE materials with high Seebeck coefficient or high power factor.

J. Zhang *et al*. JAP 110,043710 (2011)

ZT of III-V ternary (Simulation)

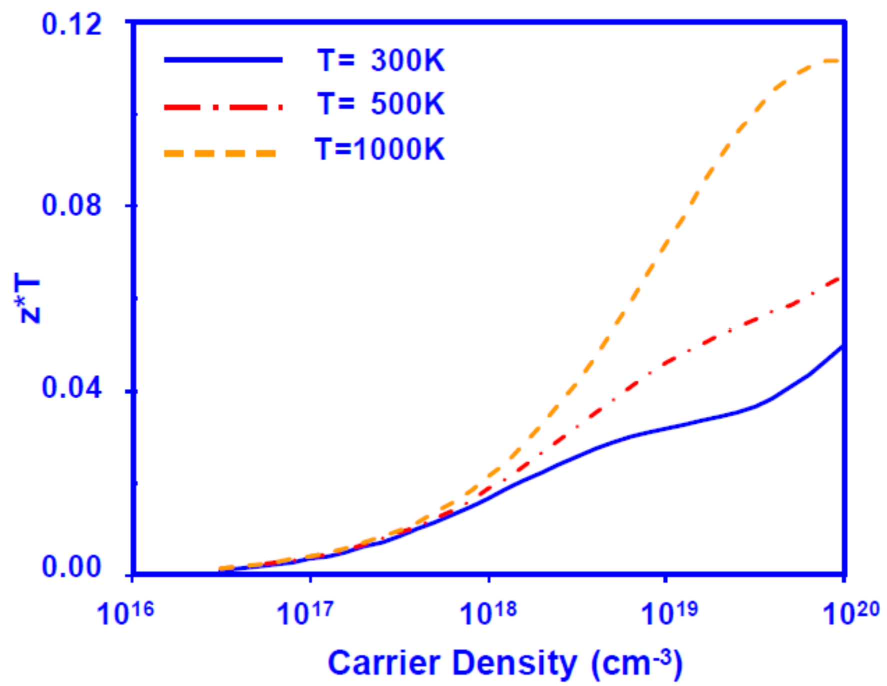

ZT of $Al_{0.4}Ga_{0.6}N$ as a function of carrier density at 300K (blue), 500 K (red), and 1000 K (yellow)

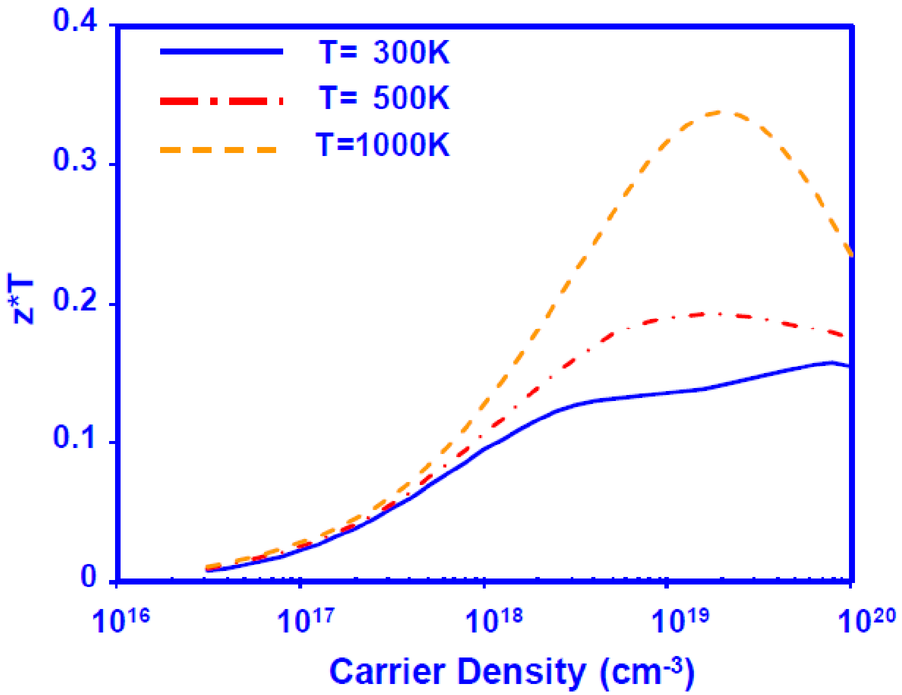

InGaN is expected to be the best TE material among III-nitride. This figure depict ZT of $In_{0.45}Ga_{0.55}N$ as a function of carrier density at 300 K (blue), 500 K (red), and 1000 K (yellow)

Hua TONG

ZT of InGaN ternary (Experiment)

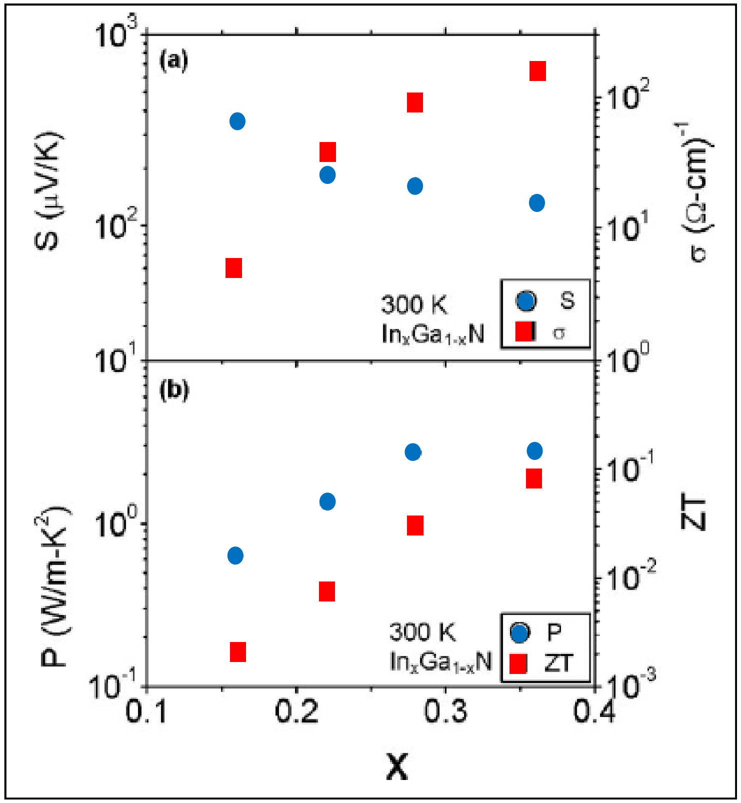

(a) Seebeck coefficient S and electrical conductivity of $In_xGa_{1-x}N$ alloys as functions of In content x. (b) Power factor $P=S^2\sigma$ and figure of merit ZT of $In_xGa_{1-x}N$ alloys as functions of In content x measured at 300 K.

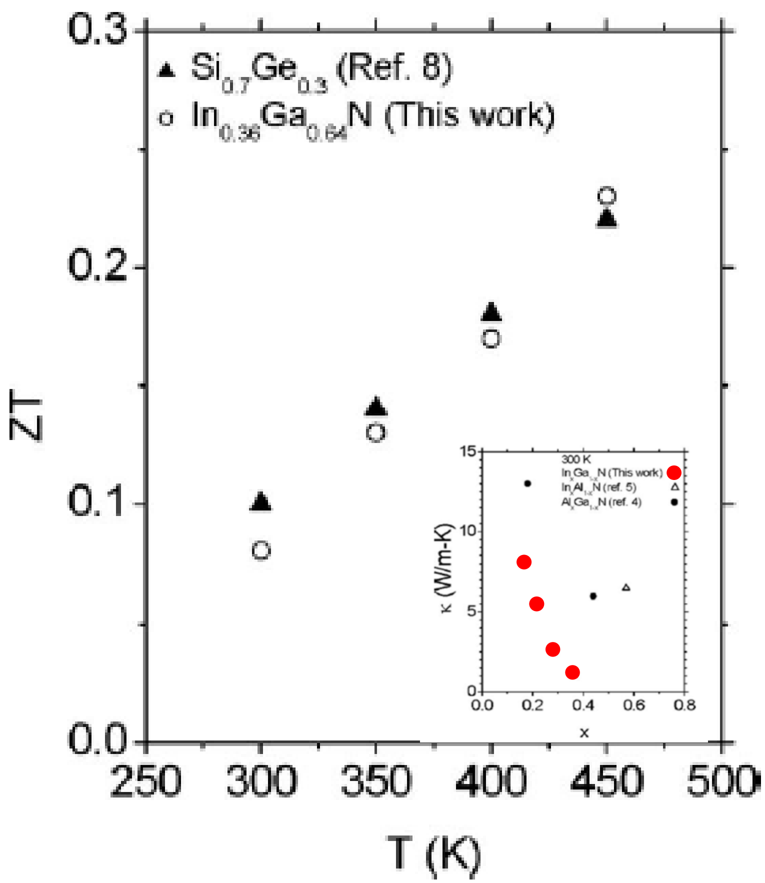

Measured ZT values of $In_{0.36}Ga_{0.64}N$ thin film from 300 to 450 K (110 nm) ZT~0.23 was obtained.

H. X. Jiang et al, Appl. Phys. Lett. 92, 042112 (2008)
Department of Physics, Kansas State University, USA

Perspective

- Nanotechnology provides great opportunity for Thermoelectric materials.
- Demonstration of high ZT materials is yet to come.

Thermoelectric Effect

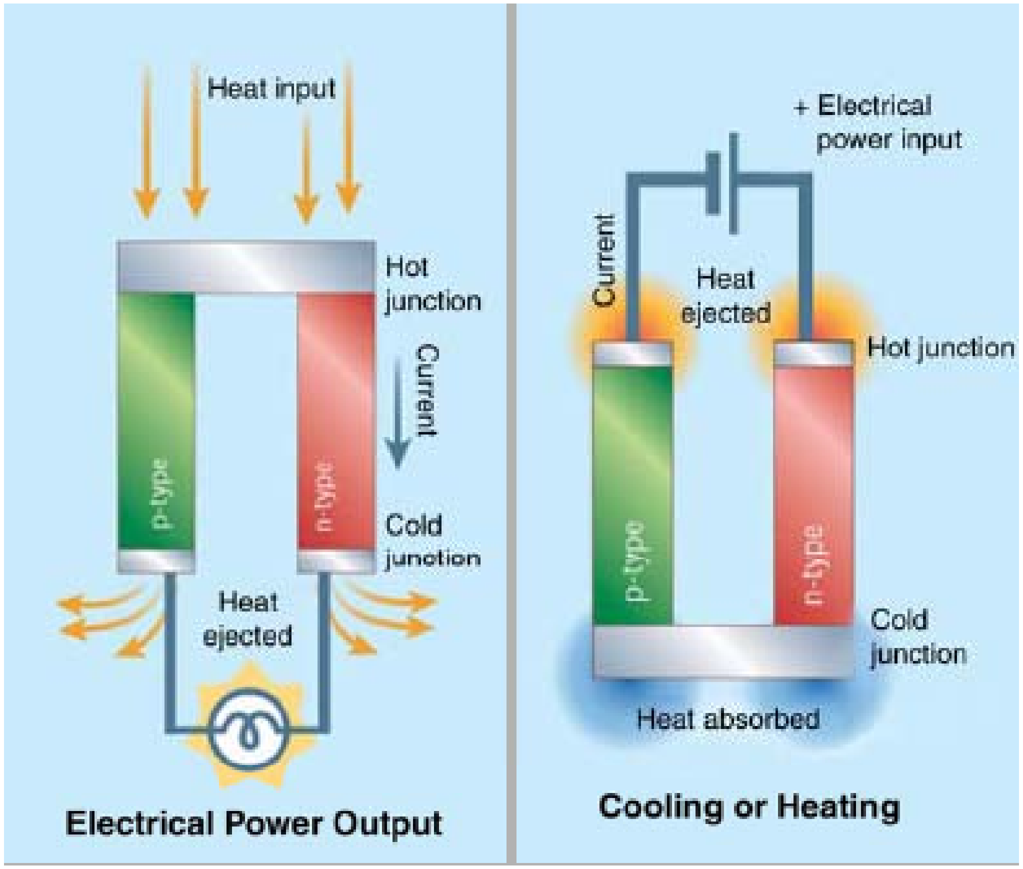

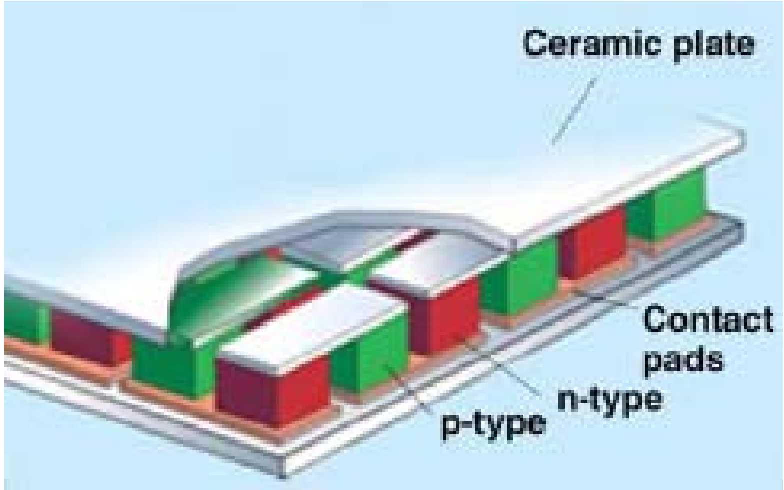

Figure of Merit & Efficiency

$$ZT = \frac{\alpha^2 \sigma T}{(\kappa_e + \kappa_{ph})}$$

$$\eta_{TE} = \eta_C \left(\frac{\sqrt{1+ZT} - 1}{\sqrt{1+ZT} + \frac{T_C}{T_H}} \right)$$

Carnot efficiency, $\eta_C = (T_H - T_C)/T_H$